AMERICAN SOCIETY FOR MICROBIOLOGY | Journal of Virology

A Highly Efficacious Herpes Simplex Virus 1 Vaccine Blocks Viral Pathogenesis and Prevents Corneal Immunopathology via Humoral Immunity

Derek J. Royer,[a] Hem R. Gurung,[a] Jeremy K. Jinkins,[b] Joshua J. Geltz,[c] Jennifer L. Wu,[b] William P. Halford,[c] Daniel J. J. Carr[a,b]

Department of Microbiology and Immunology[a] and Department of Ophthalmology,[b] University of Oklahoma Health Sciences Center, Oklahoma City, Oklahoma, USA; Department of Medical Microbiology, Immunology, and Cell Biology, Southern Illinois University School of Medicine, Springfield, Illinois, USA[c]

ABSTRACT

Correlates of immunologic protection requisite for an efficacious herpes simplex virus 1 (HSV-1) vaccine remain unclear with respect to viral pathogenesis and clinical disease. In the present study, mice were vaccinated with a novel avirulent, live attenuated virus (0ΔNLS) or an adjuvanted glycoprotein D subunit (gD-2) similar to that used in several human clinical trials. Mice vaccinated with 0ΔNLS showed superior protection against early viral replication, neuroinvasion, latency, and mortality compared to that of gD-2-vaccinated or naive mice following ocular challenge with a neurovirulent clinical isolate of HSV-1. Moreover, 0ΔNLS-vaccinated mice exhibited protection against ocular immunopathology and maintained corneal mechanosensory function. Vaccinated mice also showed suppressed T cell activation in the draining lymph nodes following challenge. Vaccine efficacy correlated with serum neutralizing antibody titers. Humoral immunity was identified as the correlate of protection against corneal neovascularization, HSV-1 shedding, and latency through passive immunization. Overall, 0ΔNLS affords remarkable protection against HSV-1-associated ocular sequelae by impeding viral replication, dissemination, and establishment of latency.

IMPORTANCE

HSV-1 manifests in a variety of clinical presentations ranging from a rather benign "cold sore" to more severe forms of infection, including necrotizing stromal keratitis and herpes simplex encephalitis. The present study was undertaken to evaluate a novel vaccine to ocular HSV-1 infection not only for resistance to viral replication and spread but also for maintenance of the visual axis. The results underscore the necessity to reconsider strategies that utilize attenuated live virus as opposed to subunit vaccines against ocular HSV-1 infection.

Herpes simplex virus 1 (HSV-1) is a highly successful human pathogen that results in approximately 40,000 new cases of severe visual impairment each year (1). In such cases, the immune response to the pathogen inadvertently mediates corneal pathology. Moreover, the morbidity associated with ocular infection results from episodic viral recrudescence (2, 3). This etiology is dependent upon reactivation of HSV-1 from latently infected neurons within the trigeminal ganglion (TG), which innervates the cornea and orofacial mucosae. Although gamma interferon (IFN-γ) and other cytokines secreted by T cells and other cornea-resident cells facilitate viral clearance in the cornea, these soluble factors also recruit neutrophils and activate macrophages replete with proteases that instigate extracellular matrix remodeling and scar formation, thereby compromising visual acuity (4–10). Furthermore, protracted inflammatory responses sustained beyond clearance of the virus contribute to corneal neovascularization (1, 11). Consequently, developing HSV vaccines that elicit robust protection against infection without enhancing the risk for corneal immunopathology is an important clinical matter as no sanctioned HSV vaccine clinical trials to date have enrolled patients with a history of ocular HSV infection (11).

Early HSV-1 vaccines against primary or recurrent ocular infection in animal models focused on the use of HSV-1/HSV-2 (HSV-1/2) glycoprotein subunits alone or in combination (12–14), likely due to the success of earlier studies that found that glycoprotein subunit vaccines were efficacious in experimental models of genital HSV-2 infection (15–17). More recent studies employing additional means to generate an immune response to viral antigens have shown that such prophylactic approaches are highly successful in terms of suppressing (i) viral replication and dissemination, (ii) establishment of latency, (iii) development of severe keratitis, and (iv) leukocyte infiltration into the cornea (18–21). Therapeutic efficacy using a replication-defective HSV-1 mutant as a vaccine to suppress reactivation of latent virus has also been reported (22). Based on the critical role that $CD8^+$ T cells play in the control of HSV-1 reactivation (23–25), another group of investigators has identified HLA-A-restricted epitopes from HSV-encoded proteins that drive $CD8^+$ T cell activation and show efficacy against ocular HSV-1 challenge in vaccinated humanized HLA-transgenic rabbits (26).

The capacity of HSV-1 vaccines to protect the visual axis from HSV-1-induced disease and pathology has seldom been quantita-

Received 18 March 2016 **Accepted** 21 March 2016

Accepted manuscript posted online 30 March 2016

Citation Royer DJ, Gurung HR, Jinkins JK, Geltz JJ, Wu JL, Halford WP, Carr DJJ. 2016. A highly efficacious herpes simplex virus 1 vaccine blocks viral pathogenesis and prevents corneal immunopathology via humoral immunity. J Virol 90:5514–5529. doi:10.1128/JVI.00517-16.

Editor: R. M. Longnecker, Northwestern University

Address correspondence to Daniel J. J. Carr, Dan-Carr@ouhsc.edu.

tively or systematically investigated. Previous investigations of HSV-1 vaccines have largely been limited to subjective clinical examinations. Only two studies have evaluated leukocyte infiltrate in corneas by immunohistochemistry following vaccination and challenge (21, 27), and that by Ghiasi et al. suggested that protection against ocular pathology correlated with preexisting HSV-1-neutralizing antibodies (27). However, focus on humoral immunity as a correlate of protection against HSV-1-induced ocular disease and latency has been eclipsed over the past decade by a focus on T cell responses to defined epitopes induced by natural infection (28, 29). Nonetheless, vaccine-induced immunologic correlates of protection have not been rigorously defined in experimental models of ocular HSV-1 infection. We hypothesize that the correlates of protection generated in response to natural infection deviate from mechanisms of prophylactic vaccine-induced immunologic protection.

In the current study, we systematically evaluated the capacity of prophylactic vaccination to protect mice from ocular HSV-1 challenge by quantitatively assessing the following: (i) viral replication, spread, and latency; (ii) cell-mediated and humoral adaptive immune responses; and (iii) corneal pathology. The efficacy of two potential prophylactic vaccines was compared, namely, a novel live attenuated HSV-1 vaccine and a glycoprotein D subunit (gD-2) vaccine similar to that used in several human clinical trials. The HSV-1 attenuation results from deletion of the nuclear localization sequence (NLS) signal peptide on infected cell protein 0 (ICP0), a decidedly pleiotropic viral efficiency regulator. In addition to being an immediate early coactivator of viral mRNA synthesis and replication, ICP0 counteracts intrinsic antiviral host cell defenses (30). Akin to many other well-characterized HSV-1/2 ICP0 mutant viruses (31–33), HSV-1 ICP0ΔNLS is an avirulent, IFN-sensitive, and immunogenic live virus. Whereas HSV-1 and HSV-2 ICP0 mutants are known to be replication competent at an elevated multiplicity of infection (MOI) (34, 35), such mutants are profoundly sensitive to type I IFN (IFN-α/β). The HSV-1 ICP0ΔNLS vaccine is here designated 0ΔNLS. A gD-2 subunit vaccine adjuvanted with alum and monophosphoryl lipid A (MPL) was used in the present study as a basis for comparing vaccine efficacy as data from the Herpevac Trial for Women showed that a similar gD-2 vaccine can elicit a modest degree of protection against HSV-1 infection and genital disease in HSV-seronegative humans (36).

Results of the current study indicate that the 0ΔNLS vaccine is superior to a gD-2 subunit vaccine in terms of its capacity (i) to elicit a highly neutralizing antibody response, (ii) to preserve corneal health, and (iii) to significantly limit virus replication, dissemination, and establishment of latency in mice ocularly challenged with HSV-1. Moreover, passive immunization with 0ΔNLS antiserum was sufficient to confer significant protection upon naive mice against ocular HSV-1 challenge with respect to viral pathogenesis and the downstream consequence of ocular herpetic disease. Consequently, we demonstrate for the first time that humoral immunity is a major correlate of protection against ocular HSV-1 infection in a mouse model.

MATERIALS AND METHODS

Mice and ocular infection. Female outbred CD-1 mice were obtained from Charles River and maintained in a specific-pathogen-free vivarium at the Dean McGee Eye Institute. This study was approved by the Oklahoma University Health Sciences Center (OUHSC) animal care and use committee (protocol number 13-019-I). Mice were anesthetized for all procedures except corneal esthesiometry by intraperitoneal (i.p.) injection of ketamine (100 mg/kg of body weight) and xylazine (6.6 mg/kg of body weight). For ocular infection challenges, corneas were inoculated with 200 or 500 PFU of HSV-1 McKrae (approximate age/weight-based 50% lethal dose [LD_{50}] for CD-1 mice) following slight epithelial debridement. High-titer challenges were conducted with 50,000-PFU inocula to determine the extent of vaccine-mediated protection. The McKrae strain was propagated and maintained at high titer as described previously (37). Mice were euthanized by cardiac perfusion with 10 to 15 ml of phosphate-buffered saline (PBS) for tissue collection and subsequent analyses.

Vaccine composition and regimen. The 0ΔNLS live attenuated virus was constructed by homologous recombination of HSV-1 strain KOS (wild-type [WT] virus) and a plasmid bearing a mutant allele of the *ICP0* gene containing an in-frame insertion of the green fluorescent protein (GFP) coding sequence between codons 104 and 105 on exon 2 (33) and a deletion of codons 500 to 507 to remove the NLS signal peptide (RPR KRR) from exon 3 (Fig. 1B). The antigenic breadth incorporated by 0ΔNLS, the recombinant construct, and the *in vitro* cellular localization of ICP0 are indicated in Fig. 1. The 0ΔNLS immunization dose was 1×10^5 PFU delivered in 10 μl of PBS. The gD-2 subunit vaccine used for this study was intended to mimic Glaxo Smith Kline's Herpevac vaccine and includes 2.5 μg of truncated gD-2_{306t} protein purified from baculovirus vector-infected High Five insect cells (Invitrogen) as previously described (32), adjuvanted with 25 μl of Imject alum (Thermo Scientific) and 10 μg of monophosphoryl lipid A (MPL) from *Salmonella enterica* serovar Minnesota (Sigma) in a 35-μl total volume. Figure 2A outlines the timeline for the experimental prime-boost-challenge regimen. Mice were 6 to 10 weeks old upon primary immunization. The doses outlined above for each vaccine were used for primary and secondary immunizations in ipsilateral rear footpads and hindquarters, respectively.

Virological assays. For *in vitro* studies (Fig. 1), wild-type and ICP0-deficient mutant viruses were quantified by plaque assay using Vero cells and the ICP0-complementing L7 cell line (38). During acute infection, the titer of lytic HSV-1 shed in the ocular tear film or recovered from infected tissue homogenates was determined via plaque assay on Vero cells (American Type Culture Collection) at the times postinfection (p.i.) indicated on the figures. Productive viral replication was evaluated in TG harvested from mice at day 5 p.i. by PCR analysis of *ICP0*, thymidine kinase (*TK*), and *gB* expression as representatives of immediate early, early, and late HSV-1 genes, respectively. Latent virus was surveyed in TG harvested from mice surviving to day 30 p.i. by PCR analysis of HSV-1 latency-associated transcript (*LAT*) expression or viral genome copy number. For PCR analysis of HSV-1 genes, RNA was isolated and converted into cDNA using iSCRIPT reverse transcription supermix (Bio-Rad) as described previously (39). Real-time PCR (RT-PCR) was performed using iTaq universal SYBR green supermix (Bio-Rad). Reported HSV-1 lytic gene data are relative to data for uninfected (UI) controls and standardized to murine phosphoglycerate kinase 1 (*PGK1*) expression using the $2^{-\Delta\Delta CT}$ (where C_T is threshold cycle) method. Similarly, *LAT* expression data are relative to data of UI controls and standardized by the geometric mean of murine glyceraldehyde-3-phosphate dehydrogenase (*GAPDH*) and eukaryotic translation elongation factor 1 epsilon-1 (*Eef1e1*) or β-actin expression. Table 1 gives the primer sequences. For HSV-1 genome copy number analysis, DNA was carefully isolated and purified from TG, and quantitative PCR was performed with GoTaq PCR reagents (Promega) and a proprietary HSV-1-specific primer/reporter-probe mix (De novo Biotechnology). A CFX Connect thermocycler (Bio-Rad) was used for all PCR experiments.

Corneal pathology. Edema and mechanosensation in healthy and HSV-1-infected corneas of vaccinated and naive mice were measured using a Corneo-Gage Plus digital pachymeter (Sonogage) and a handheld Cochet-Bonnet esthesiometer (Luneau Technology), respectively, as previously described (37, 40). Labeling, imaging, and analysis of vasculature in cornea flat mounts were performed using an Olympus FV500 confocal

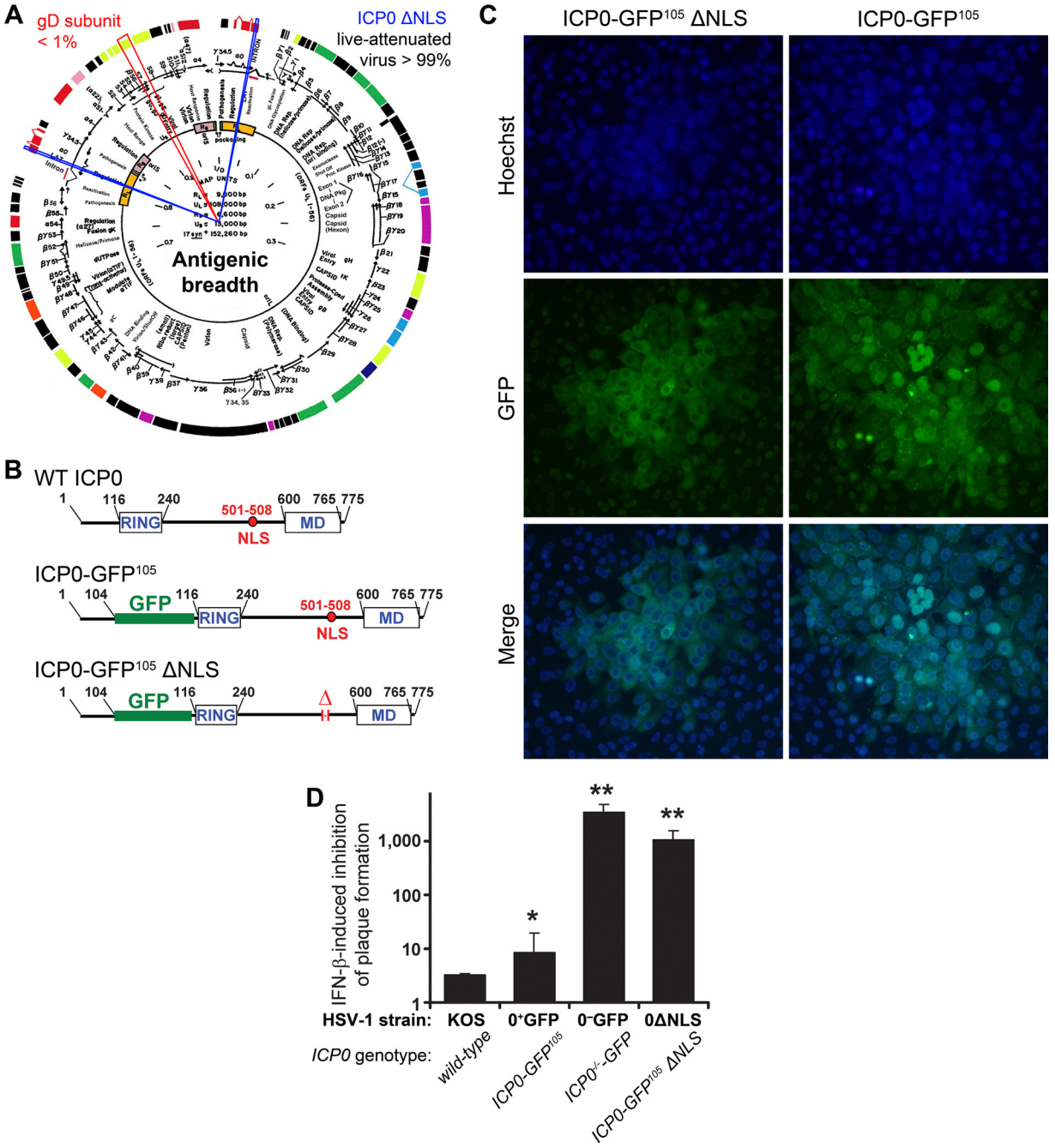

FIG 1 Attenuated virus vaccine. (A) The ICP0 ΔNLS live attenuated HSV-1 vaccine (0ΔNLS) maintains >99% of the antigenic breadth of HSV-1 relative to the wild-type virus. In contrast, the glycoprotein D (gD) subunit vaccines tested in numerous clinical trials represents <1% of the viral proteome (red cutout). Blue cutouts on each copy of the *ICP0* gene denote the loci deleted from the HSV-1 0ΔNLS vaccine strain. (B) The upper panels show a schematic of the ICP0 protein encoded by wild-type (WT) HSV-1, which includes an N-terminal RING finger motif, nuclear localization signal (NLS), and a C-terminal multimerization domain (MD). A schematic of the full-length, GFP-tagged ICP0 protein referred to here as ICP0-GFP^{105}, which contains an insertion of the green fluorescent protein (GFP) coding sequence between codons 104 and 105 of the *ICP0* gene, is shown in the middle. At bottom is a schematic of the GFP-tagged ICP0 protein encoded by HSV-1 0ΔNLS, ICP0ΔNLS-GFP^{105}, which bears a deletion in amino acids 501 to 508 of ICP0 and removes the protein's canonical NLS (RPRKRR). (C) Comparison of single plaques of HSV-1 0ΔNLS and HSV-1 ICP0-GFP^{105} in a monolayer of Vero cells as photographed at 30 h postinoculation under conditions of illumination that show the nuclear dye Hoechst 33342, the GFP-tagged ICP0 proteins made by each virus (ICP0 with or without the NLS), or a merge of both. (D) Relative IFN-β sensitivity of WT HSV-1, HSV-1 ICP0-GFP^{105}, HSV-1 0ΔNLS, or HSV-1 ICP0$^{-/-}$-GFP (ICP0-null mutant) to inhibition of plaque formation in Vero cell monolayers treated with 200 U/ml IFN-β. Specifically, the column graph represents the mean ± standard deviation of the ratio of plaques that were formed when each virus was plated on ICP0-complementing L7 cells to define the actual titer versus Vero cells treated with 200 U/ml IFN-β. In prior studies, all viruses that exhibit a >500-fold inhibition of plaque formation in IFN-β-treated Vero cells have proven to be avirulent *in vivo*.

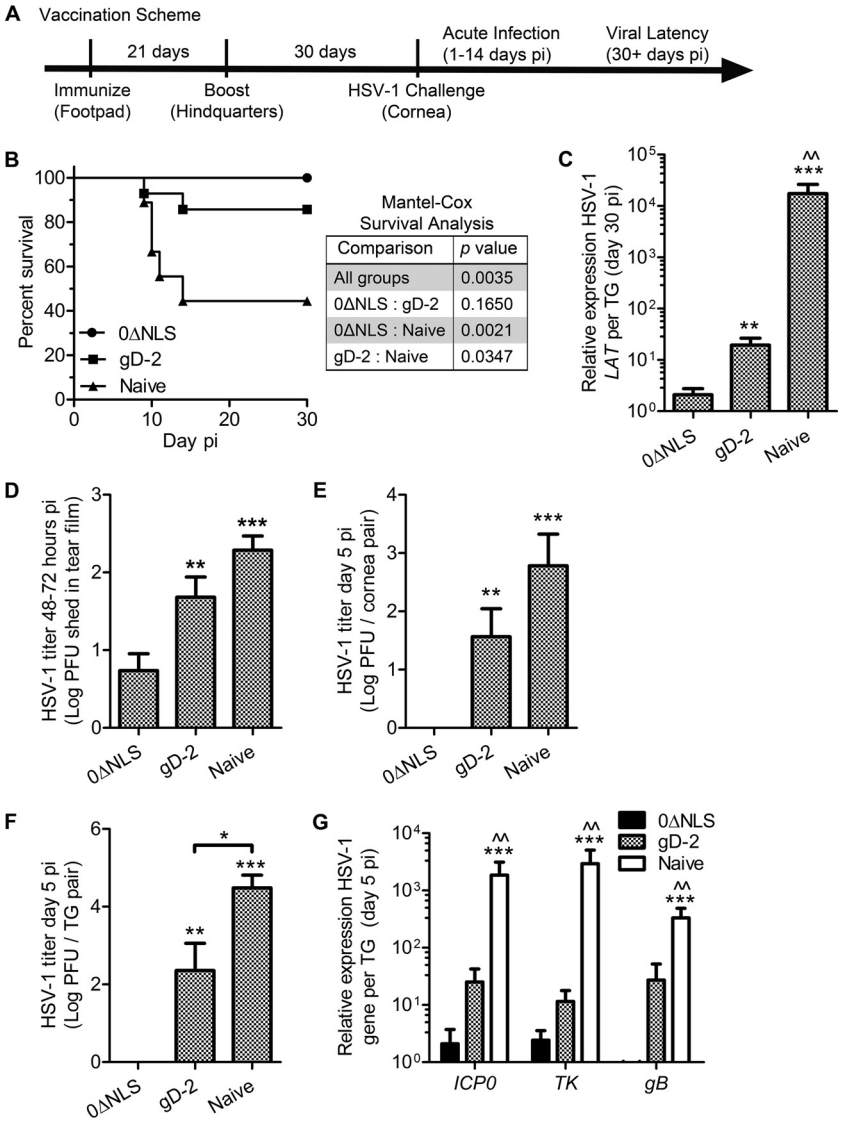

FIG 2 Vaccination scheme and outcome measures. (A) Timeline depicting the vaccination scheme and HSV-1 challenge. (B) Animal survival following HSV-1 infection ($n = 9$ to 14 mice per group). A Mantel-Cox test was used to compare differences in survival outcomes (P values are given in the inset table). (C) Animals were euthanized at day 30 p.i. to assess viral latency in the TG by expression of *LAT* relative to that of *GAPDH* (glyceraldehyde-3-phosphatase dehydrogenase) and eukaryotic translation elongation factor 1 epsilon-1 or β-actin expression ($n = 7$ to 24 TG per group; 4 to 5 independent experiments). Differences in *LAT* expression levels were determined by nonparametric Kruskal-Wallis ANOVA with Dunn's multiple comparison tests. Viral burden was assessed by plaque assay to measure HSV-1 shedding in the ocular tear film ($n = 15$ to 21 mice/group; 5 independent experiments) (D), excised corneas (E), and TG ($n = 5$ to 7 mice per group; 3 independent experiments) (F). Differences in HSV-1 titers were determined by one-way ANOVA with Student-Newman-Keuls multiple comparison tests. (G) PCR analysis of the HSV-1 genes infected cell protein 0 (*ICP0*), thymidine kinase (*TK*), and glycoprotein B (*gB*) in the TG at day 5 p.i. relative to phosphoglycerate kinase 1 (*PGK1*) expression ($n = 10$ TG per group; 2 independent experiments). Differences in lytic viral gene expression were determined by nonparametric Kruskal-Wallis ANOVA with Dunn's multiple comparison tests. Significance thresholds are designated as follows: *, $P < 0.05$; **/^^, $P < 0.01$; ***, $P < 0.001$. Significant differences in results for the 0ΔNLS- and the gD-2-immunized groups are shown as asterisks and carets, respectively.

microscope and MetaMorph Imaging Suite (Molecular Devices) as described previously (41). Multidimensional renderings of confocal images were developed using Imaris software (Bitplane).

On the indicated days p.i. (Fig. 3), a masked observer examined mouse eyes through a Kowa SL14 portable slit lamp biomicroscope to score pathology. Corneal opacification was rated on a scale of 1 to 6, where 1 indicates mild stromal haze, 2 indicates moderate opacity, 3 indicates moderate opacity with regional dense opacity, 4 indicates diffuse dense opacity, 5 indicates diffuse dense opacity with corneal ulcer, and 6 indicates corneal perforation.

Flow cytometry. Submandibular lymph nodes (MLN) were harvested from vaccinated and naive mice at day 5 p.i. for analysis by flow cytometry. Briefly, MLN pairs were macerated into single-cell suspensions in RPMI 1640 medium containing 10% heat-inactivated fetal bovine serum (FBS), 1× antibiotic/antimycotic, and 10 μg/ml gentamicin (Gibco), i.e., complete medium. Corneas were digested in 2.0 mg/ml type 1 collagenase (Sigma) as described previously (37). Cell suspensions were filtered through 40-μm-pore-size mesh, immunolabeled with eBioscience or AbD Serotec antibodies, washed, and fixed as previously described (37). Spleens were harvested and processed as described previously (37). Samples were analyzed on a MacsQuant flow cytometer (Miltenyi Biotech).

Virus neutralization assay. Blood was collected from the facial vein of naive and vaccinated mice prior to secondary vaccination and challenge (Fig. 2A) and fractionated using Microtainer serum separator tubes (Bec-

TABLE 1 Primer sequences

Primer name[a]	Sequence
β-Actin FWD	5′-CTTCTACAATGAGCTGCGTGTG-3′
β-Actin REV	5′-TTGAAGGTCTCAAACATGATCTGG-3′
Eef1e1 FWD	5′-GCAGAAGAAAAGGCAATGGT-3′
Eef1e1 REV	5′-AGGCCGTAGTACAGCAGGAT-3′
GAPDH FWD	5′-AGAATTGACAAACGGGACCT-3′
GAPDH REV	5′-GGAGGAGCAGAGAGCTTGAC-3′
PGK1 FWD	5′-CTGACTTTGGACAAGCTGGACG-3′
PGK1 REV	5′-GCAGCCTTGATCCTTTGGTTG-3′
HSV-1 ICP0 FWD	5′-GGTCCCCACTGACTCATACG-3′
HSV-1 ICP0 REV	5′-ATCCCGACCCCTCTTCTTC-3′
HSV-1 TK FWD	5′-ATACCGACGATCTGCGACCT-3′
HSV-1 TK REV	5′-TTATTGCCGTCATAGCGCGG-3′
HSV-1 gB FWD	5′-TCTGCACCATGACCAAGTG-3′
HSV-1 gB REV	5′-TGGTGAAGGTGGTGGATATG-3′
HSV-1 LAT FWD	5′-CCCTCGTCTCCTGTGATTCT-3′
HSV-1 LAT REV	5′-GGGAGACAGAAACAGGAACAT-3′

[a] Eef1e1, eukaryotic elongation factor 1 epsilon-1; FWD, forward; GAPDH, glyceraldehyde-3-phosphate dehydrogenase; gB, glycoprotein B; HSV-1, herpes simplex virus 1; ICP0, infected cell protein 0; LAT, latency-associated transcript; PGK1, phosphoglycerate kinase 1; REV, reverse; TK, thymidine kinase.

ton Dickinson). Blood was collected at 18 ± 1 days after primary immunization (primary) and 26 ± 2 days following the secondary immunization (boost). Serum samples were combined 1:25 with complete medium in microtiter plates and serially diluted 2-fold (total volume [V_{total}], 200 μl/well). Next, guinea pig complement (Rockland Immunochemicals) diluted 1:20 in complete medium containing 2.85×10^5 PFU/ml HSV-1 McKrae was added to each well (10 μl). The plate was gently mixed and incubated (at 37°C in 5% CO_2) for 2 h. Confluent Vero cells were subsequently exposed to 100 μl of each virus-serum dilution for 1 h, decanted, and incubated for 24 h in complete medium. Neutralization titers are reported as the reciprocal serum dilution at which a 50% reduction in cytopathic effect (CPE) was observed.

Western blotting. Protein from freeze-thawed healthy and HSV-1-infected Vero cells was isolated, measured, resolved on 4 to 20% Tris-glycine polyacrylamide gels (20 μg/sample), and transferred as described previously (40). Nitrocellulose membranes were blocked in 5% bovine serum albumin (BSA) and subsequently exposed to naive, immunized, or immunoglobulin (Ig)-depleted mouse serum (diluted 1:500) overnight at 4°C. Chemiluminescent detection and imaging were achieved as described previously (40). Apparent molecular weights were determined using a BenchMark prestained ladder (Invitrogen).

In another experiment, 12 μg of protein from uninfected Vero cells or Vero cells infected with HSV-1 (KOS strain), HSV-2 (strain MS from the American Type Culture Collection), or HSV-1 ΔgD (gK6) or from HSV-1 gD2-expressing Vero cells (TR-gD2) was resolved in an 8% denaturing polyacrylamide gel and transferred to nitrocellulose membranes. PageRuler Plus molecular weight markers (Thermo Scientific) were electrophoresed to determine apparent molecular weight resolution for each gel. Membranes were blocked using phosphate-buffered saline (PBS) containing 5% nonfat dry milk and were incubated overnight at 4°C in PBS containing 0.1% Tween 20 (PBS-T) plus 5% nonfat dry milk containing a 1:5,000 dilution of mouse serum. Following incubation with mouse antibody, the membranes were washed four times with PBS-T and incubated with goat anti-mouse infrared fluorescent dye (IRDye 800CW; Li-Cor Bioscience) for 1 h at 4°C. The membranes were then washed three times with PBS-T and rinsed once in PBS to remove residual Tween 20. The membranes were then scanned for fluorescence using an Odyssey infrared imaging system (Li-Cor Bioscience).

Passive immunization. Terminal cardiac puncture of deeply anesthetized naive and fully vaccinated mice was used to obtain volumes of serum required for passive immunization experiments. Pooled 0ΔNLS, gD-2, or naive serum was administered i.p. (250 μl) to naive CD-1 mice 24 h prior to HSV-1 challenge. For experimental controls, serum was Ig depleted using protein L-agarose columns (Pierce/Thermo Scientific) according to the manufacturer's directions and reconcentrated via dialysis spin columns (Amicon/Millipore).

Statistical analysis. GraphPad Prism, version 5, was used for statistical analysis. All data reflect means ± standard errors of the means (SEM). Student's *t* tests were used when appropriate. For comparisons of several groups, one-way analyses of variance (ANOVAs) with Student-Newman-Keuls multiple-comparison test were used to appraise parametric data; nonparametric data were evaluated using Kruskal-Wallis ANOVAs with Dunn's multiple comparison tests; two-way ANOVAs with Bonferroni posttests were employed to assess data with two independent variables. Mantel-Cox tests were utilized for survival curve analysis.

RESULTS

Vaccine composition and interferon sensitivity. Live attenuated viruses such as 0ΔNLS maintain a majority of a pathogen's natively encoded antigens in comparison to glycoprotein subunits, which individually reflect only a fraction of the antigenic breadth (Fig. 1A). We investigated the potential use of 0ΔNLS as a prophylactic vaccine administered peripherally in comparison to a gD-2 subunit vaccine, similar in composition to that used in human clinical trials (36). The 0ΔNLS attenuation results from deletion of the NLS signal peptide domain on exon 3 of ICP0. Importantly, HSV-1 0ΔNLS encodes a nearly full-length ICP0 protein but features an in-frame GFP insertion to facilitate identification of intracellular localization and an in-frame deletion that removes amino acids 501 to 508 which encode the canonical NLS, RPRKRR (Fig. 1 B, bottom). The virulence of 0ΔNLS is severely diminished as ICP0 remains in the cytoplasm and cannot translocate to the nuclear compartment (Fig. 1C) to promote viral mRNA synthesis or counteract IFN-α/β-driven innate and intrinsic cellular defenses (30, 42).

HSV-1 ICP0 and HSV-2 ICP0 mutants are profoundly sensitive to repression by IFN-β *in vitro* and correspondingly avirulent in both immunocompetent and immunocompromised animal models, such as SCID and RAG2$^{-/-}$ mice (31, 32, 43). Accordingly, we evaluated the sensitivity of HSV-1 0ΔNLS to inhibition by IFN-β. Consistent with past results, HSV-1 strain KOS (i.e., the parental strain of the 0ΔNLS mutant) expressing the wild-type (WT) ICP0 protein exhibited a modest 3-fold reduction in plaque formation efficiency on IFN-β-treated Vero cells relative to that of ICP0-complementing L7 cells (Fig. 1D). Similarly, HSV-1 ICP0-GFP^{105}, a GFP-tagged pseudo-WT variant (Fig. 1B, middle), exhibited a 9-fold reduction in efficiency of plaque formation in the same assay (Fig. 1D). In contrast, an ICP0-null HSV-1 mutant encoding GFP on the *ICP0* locus (schematic not shown) was exceedingly sensitive to IFN-β and showed a reduction in plaque formation efficiency in excess of 1,000-fold (Fig. 1D). Notably, HSV-1 0ΔNLS was 98% as sensitive to inhibition by IFN-β as the ICP0-null mutant (Fig. 1D). In the absence of IFN-β treatment, HSV-1 0ΔNLS exhibits only a 14-fold ± 5-fold reduction in the efficiency of plaque formation on Vero cells relative to that of the ICP0-complementing cell line (data not shown). These findings are consistent with the phenotype of HSV-2 0ΔNLS (31). Therefore, like many other HSV-1 ICP0 mutant viruses, 0ΔNLS is profoundly sensitive to repression by IFN-β.

Vaccine efficacy relative to viral pathogenesis. The pathogenesis of HSV-1 infection can be categorized into acute (days 1 to 14 p.i.) and latent (>30 days p.i.) infection based on clearance of

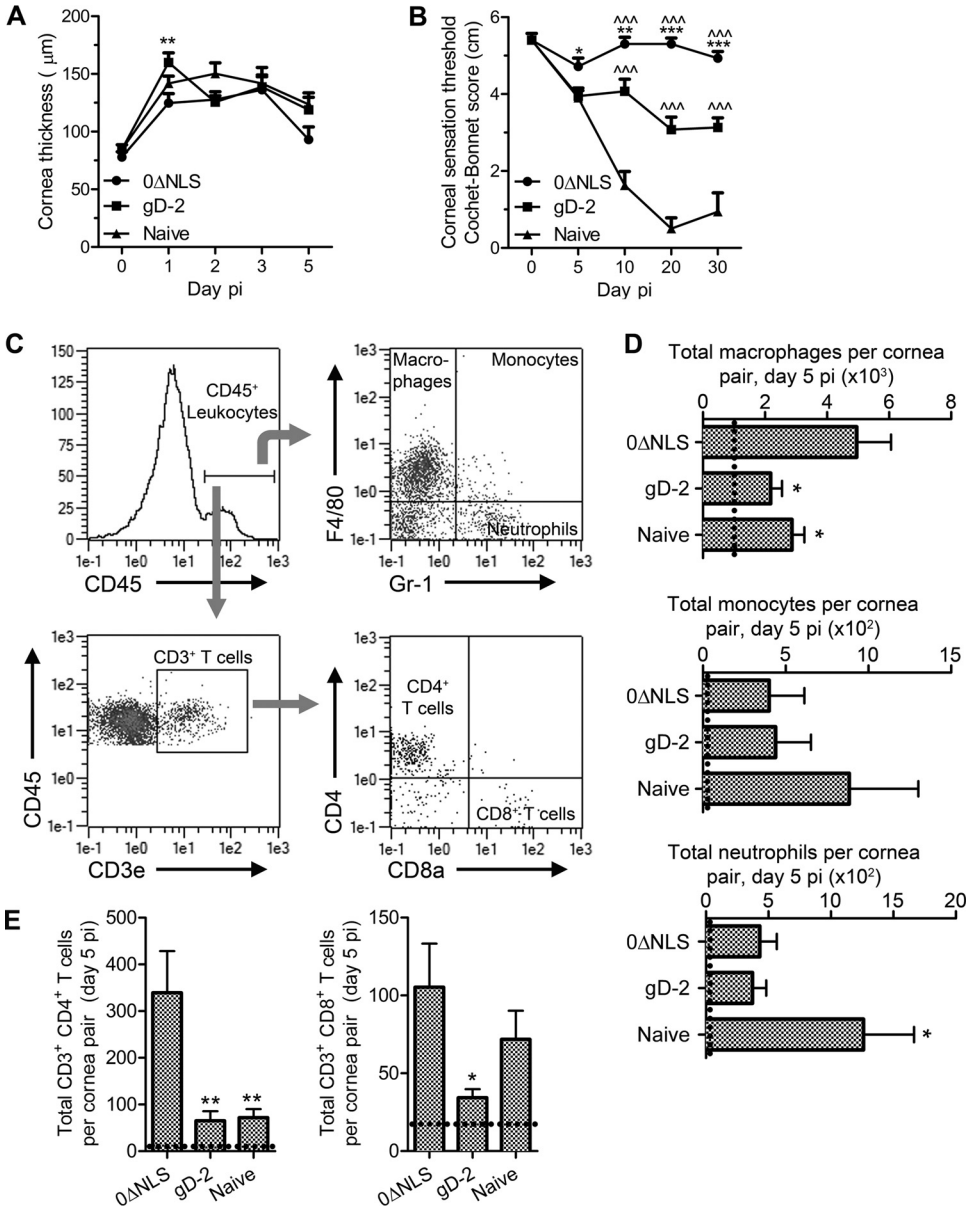

FIG 3 Vaccine-mediated protection from corneal pathology. (A) Central corneal thickness was evaluated via ultrasound pachymetry to assess corneal edema during the early acute phase post-HSV-1 challenge in immunized and naive mice ($n = 10$ to 20 corneas/group/time point; 2 to 3 independent experiments). (B) Central corneal sensation was measured longitudinally by Cochet-Bonnet esthesiometry in immunized and naive mice as a functional measure of vaccine-mediated protection from corneal denervation following HSV-1 infection ($n = 10$ to 30 corneas/group/time point; 4 independent experiments). For panels A and B, two-way ANOVAs with Bonferroni posttests were utilized to determine statistical differences. (C) Representative composite depicting gating strategy for flow cytometric analysis of cornea-infiltrating leukocytes. (D) Quantification of cornea-infiltrating myeloid cells, including macrophages ($F4/80^+$ $Gr\text{-}1^-$), monocytes ($F4/80^+$ $Gr\text{-}1^+$), and neutrophils ($F4/80^-$ $Gr\text{-}1^+$). (E) Quantification of cornea-infiltrating $CD4^+$ and $CD8^+$ T cell subsets. For panels D and E, $n = 10$ to 15 mice/group with 4 to 5 independent experiments; dashed lines indicate average values for uninfected controls ($n = 2$). Differences in cell populations were determined by one-way ANOVA with Student-Newman-Keuls multiple comparison tests. Significance thresholds for all panels are indicated as follows: *, $P < 0.05$; **, $P < 0.01$; ***/^^^, $P < 0.001$. Significant differences in results relative to the gD-2-immunized and naive groups are shown as asterisks and carets, respectively.

actively replicating virus in an immunologically naive animal (Fig. 2A). Mice vaccinated with 0ΔNLS or the gD-2 subunit vaccine were less susceptible to challenge with a highly neurovirulent strain of HSV-1 (McKrae) than naive animals in terms of cumulative survival (Fig. 2B). Animals vaccinated with 0ΔNLS displayed a high degree of resistance in comparison to gD-2-vaccinated animals with regard to establishment of viral latency (Fig. 2C) defined by detection of *LAT* by RT-PCR in TG samples at day 30 p.i. Though gD-2-vaccinated animals exhibited significantly reduced *LAT* expression in the TG compared to that in naive animals, *LAT* was diminished further to nearly undetectable levels in 0ΔNLS-vaccinated mice challenged with age/weight-matched median lethal dose inocula (200 to 500 PFU per eye; LD_{50}) (Fig. 2C).

Protection against viral shedding, replication, and dissemination was observed early following HSV-1 challenge (≤3 to 5 days p.i.) in 0ΔNLS-vaccinated mice relative to that in other experimental groups (Fig. 2D to G). Specifically, virus shed from the ocular tear film during the first 2 to 3 days p.i. in 0ΔNLS-vaccinated mice was significantly reduced in comparison to that in gD-2-vaccinated or naive animals (Fig. 2D). Furthermore, no virus was detectable by plaque assay in cornea samples from 0ΔNLS-vaccinated animals by day 5 p.i. (Fig. 2E). Correspondingly, no infectious virus was detectable in the TG of 0ΔNLS-vaccinated animals at day 5 p.i. by plaque assay, whereas virus was concurrently readily detectable in TG samples from gD-2-vaccinated and naive mice (Fig. 2F). As a more sensitive interpretation of acute viral replication and neuroinvasion, RT-PCR was used to quantify viral gene expression in TG samples at day 5 p.i. (Fig. 2G). Expression levels in 0ΔNLS-vaccinated mice were 10 to 1,000 times lower than those in gD-2-vaccinated and naive mice, respectively, for *ICP0* and *TK* (Fig. 2G). Moreover, the late viral gene product required for progeny virion assembly (*gB*) was not detected in TG from 0ΔNLS-vaccinated mice (Fig. 2G), suggesting a highly restricted and nonproductive infection of the peripheral nervous system following mucosal HSV-1 challenge.

Vaccine efficacy relative to ocular pathology. Infectious or traumatic insults involving the cornea can compromise its immunoprivileged status and consequently permit substantial pathological sequelae, including leukocyte infiltration, corneal edema, hypoesthesia (sensation loss), and neovascularization. Following HSV-1 infection in mice, pathological corneal edema and neovascularization ensue commensurate with epithelial thinning within geographic corneal lesions (1, 2, 44). Similar to corneal neovascularization, hypoesthesia is a hallmark of herpes stromal keratitis in mice and humans and results from denervation of the epithelium-associated subbasal mechanosensory nerve fibers (40, 45, 46). It was of interest to determine whether vaccinated mice could be phenotypically categorized based on quantifiable measurements of tissue pathology.

Corneal edema (Fig. 3A) and neovascularization were evaluated at specified times following the LD_{50} challenge via ultrasound pachymetry and confocal microscopy, respectively. Mice from all experimental groups developed corneal edema following HSV-1 challenge. However, corneas from gD-2-vaccinated mice were significantly more edematous than those from their 0ΔNLS-vaccinated counterparts at 24 h p.i. Measurements of corneal edema were not significantly different between any groups on subsequent days p.i. Nonetheless, corneal thickness returned to near-baseline levels by day 5 p.i. exclusively in 0ΔNLS-vaccinated mice (Fig. 3A), thus correlating with viral clearance (Fig. 2E). Corneal neovascularization, defined as invasion and development of blood and lymphatic vessels in the normally avascular cornea, was precluded in directly immunized mice receiving either 0ΔNLS or gD-2 vaccines, as determined by assessment at day 30 p.i. (data not shown). However, naive mouse corneas developed substantial corneal neovascularization (data not shown) following HSV-1 infection (1, 41).

Deficiencies in corneal sensation are commonly gauged clinically by assessing the corneal blink reflex. Accordingly, we measured corneal sensation with a Cochet-Bonnet esthesiometer at different times p.i. The results show a progressive corneal sensation loss in naive, nonvaccinated mice out to day 30 p.i. (Fig. 3B), consistent with previous findings (40). Corneal sensation was completely preserved in 0ΔNLS-vaccinated mice at all times p.i. with one exception: a nonsignificant 10% drop and subsequent recovery of sensation were noted around day 5 p.i. in 0ΔNLS-vaccinated mice (Fig. 3B). In comparison, the sensation threshold gradually diminished by 25 and 40% without recovery in gD-2-vaccinated mice between day 5 and day 30 p.i., respectively (Fig. 3B). Therefore, 0ΔNLS-vaccinated mice maintain corneal function in terms of tactile sensation, whereas gD-2 subunit-vaccinated animals lose an important feature critical for corneal health and integrity.

Leukocyte infiltration into the cornea upon acute infection contributes to viral clearance but is also suspect in mediating tissue pathology. Flow cytometry was utilized to determine the impact on myeloid and T cell infiltration into corneas of vaccinated and naive mice following HSV-1 challenge using CD45, F4/80, Gr-1, CD3e, CD4, and CD8 antigens to identify unique cell types (Fig. 3C to E). Comparing all groups, no differences were observed in the total numbers of infiltrating $CD45^+$ leukocytes (data not shown). However, it was noted that the 0ΔNLS-vaccinated mice had significantly more $F4/80^+$ $Gr\text{-}1^-$ macrophages in the cornea than the other groups surveyed (Fig. 3D). No differences were noted in infiltrating $F4/80^+$ $Gr\text{-}1^+$ monocytes, which are associated with acute viral clearance (47). Neutrophil ($F4/80^-$ $Gr\text{-}1^+$) infiltration was appreciably limited in both vaccinated groups compared to that in naive animals (Fig. 3D). T cell infiltration was elevated in corneas of 0ΔNLS-vaccinated mice relative to that in gD-2-vaccinated mice for both $CD4^+$ and $CD8^+$ subsets (Fig. 3E), whereas similar numbers of $CD8^+$ but not $CD4^+$ T cells were observed in 0ΔNLS-vaccinated and naive animals (Fig. 3E). Despite the leukocyte infiltration into corneas of 0ΔNLS-vaccinated mice, these animals are refractory to corneal hypoesthesia and neovascularization.

Capacity of vaccine-mediated protection. Efficacies of vaccine-mediated protection against infection are often proportional only to a certain reciprocal challenge dose threshold (48), as has been observed with breakthrough varicella (49). To further demonstrate the extent of immunologic protection elicited by the 0ΔNLS vaccine, immunized mice were challenged with a 100-fold-higher viral inoculum than that described above (50,000 PFU/cornea; 100× LD_{50}) and assessed for sensitivity to infection (Fig. 4). In terms of cumulative survival, 100% (8/8) of 0ΔNLS-vaccinated mice survived the viral challenge whereas 50% (4/8) and 12.5% (1/8) of gD-2 subunit-vaccinated and nonvaccinated mice, respectively, survived (Fig. 4A). Similar to mice challenged at a lower infectious dose, surviving 0ΔNLS-vaccinated mice infected with 50,000 PFU of HSV-1 expressed significantly less *LAT* in the TG than gD-2 subunit-vaccinated or nonvaccinated mice at day 30 p.i. (Fig. 4B).

Corneal opacity measurements were conducted to gauge the generalized health of the cornea in challenged mice. Both gD-2 subunit- and 0ΔNLS-vaccinated mice displayed measurable moderate opacity of the cornea at day 5 p.i. (Fig. 4C). However, by day 30 p.i. in surviving animals, the gD-2 subunit-vaccinated and nonvaccinated mice had significantly higher opacity scores than the 0ΔNLS-vaccinated mice, in which the relative opacity remained similar to that of the day 5 p.i. time point (Fig. 4C). Of interest, the central cornea of the 0ΔNLS-vaccinated mice was completely transparent with minimal vessel obscuration, whereas the peripheral cornea remained moderately opaque. This phenotype was not observed in the other two groups. At day 5 p.i., the

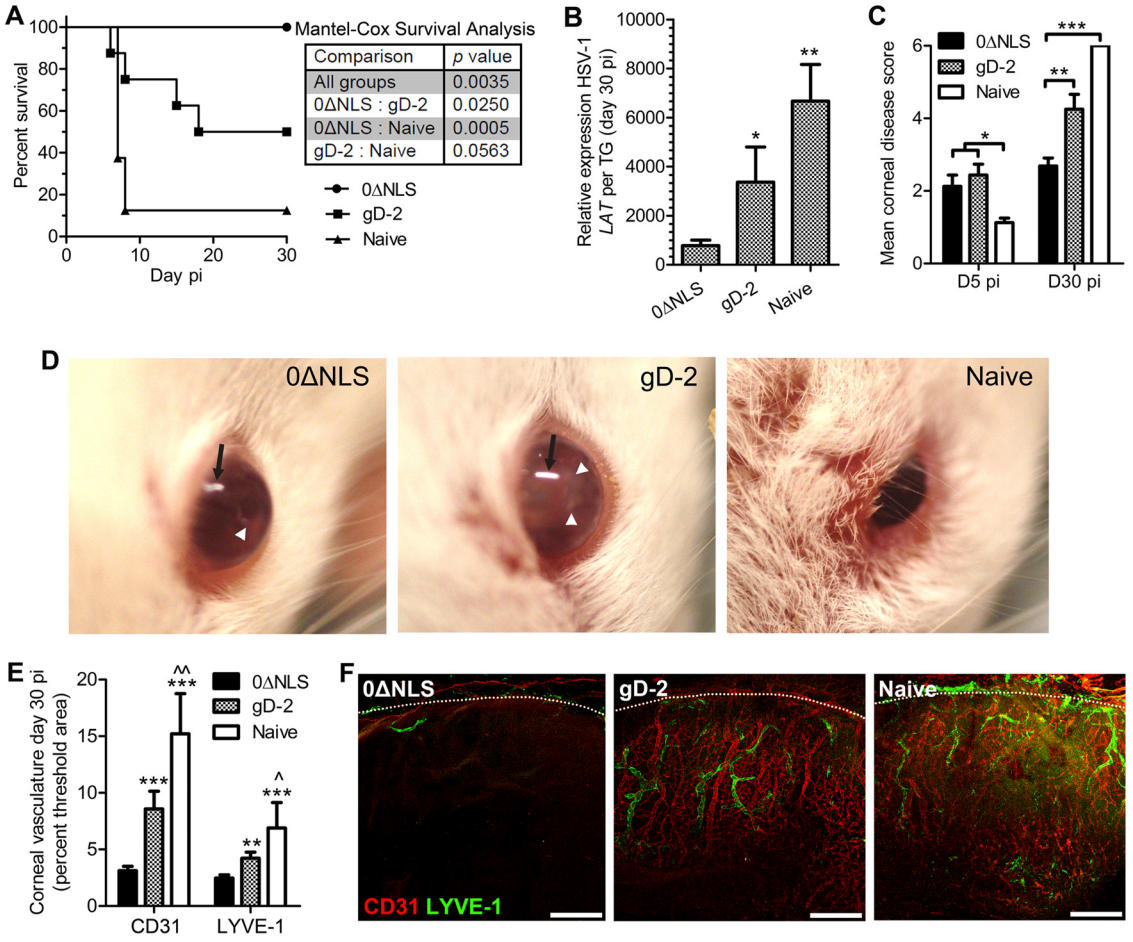

FIG 4 Capacity of vaccine-mediated protection against a high-titer challenge inoculum. Vaccinated and naive mice were ocularly challenged with 50,000 PFU of HSV-1 and assessed for cumulative survival (A), viral latency in the TG at day 30 p.i. (B), and corneal opacity at days 5 and 30 p.i. (C). (D) Representative photographs of mice at day 5 p.i. showing signs of clinical disease. Black arrows indicate light reflection artifact, and white arrowheads pinpoint areas of corneal opacification; differences in the central versus peripheral opacification can be appreciated by comparing 0ΔNLS- and gD-2-immunized mice. Corneal neovascularization was assessed at day 30 p.i. in all groups. (E) Pathological corneal neovascularization evaluated by confocal microscopy in fixed immunolabeled cornea flat mounts taken from mice at day 30 p.i. The total area of $CD31^+$ blood vessels and $LYVE\text{-}1^+$ lymphatic vessels in the cornea quantified using MetaMorph software is shown. (F) Representative images of corneal neovascularization (magnification, ×10; scale bar, 200 μm). Dotted lines indicate the limbus, the naturally vascularized anatomic boundary circumscribing the healthy cornea. Data reflect two independent experiments with a total of 8 mice per group at days 0 and 5 p.i. and with 1 naive and 4 gD-2- and 8 0ΔNLS-immunized mice at day 30 p.i. Data shown exclusively reflect results with a 100× LD_{50} dose; data in all other figures reflect the standard LD_{50} challenge inoculum. Statistical differences were determined by one-way ANOVA with Student-Newman-Keuls multiple comparison tests for panel C and E and as described in the legend of Fig. 2 for *LAT* expression. Significance thresholds for all panels are indicated as follows: */^, $P < 0.05$; **/^^, $P < 0.01$; ***, $P < 0.001$. Unless indicated otherwise, significant differences in results relative to the 0ΔNLS- and gD-2-immunized groups are shown as asterisks and carets, respectively.

difference in appearance of infected mice was notable between 0ΔNLS-vaccinated mice and the gD-2 subunit-vaccinated and nonvaccinated mice (Fig. 4D). Signs of blepharitis and periocular lesions were evident in the gD-2 subunit-vaccinated mice and nonvaccinated group but were absent in the 0ΔNLS-vaccinated animals infected with HSV-1.

Given the dramatic changes in corneal opacity in vaccinated and nonvaccinated mice between days 5 and 30 p.i., we subsequently investigated corneal neovascularization at day 30 p.i. Similar to the opacity scores at day 30 p.i., there was a substantial difference in neovascularization of the cornea (Fig. 4E and F). The gD-2 subunit-vaccinated and nonvaccinated mice exhibited notably more blood and lymphatic vessels in the cornea than 0ΔNLS-vaccinated animals (Fig. 4E and F). Therefore, in terms of efficacy, the 0ΔNLS vaccine was found to be far superior to the gD-2 subunit vaccine against a high-titer challenge inoculum and warranted additional study to evaluate and extrapolate the immunologic correlate(s) of protection in the vaccinated host.

Immunologic correlates of vaccine-mediated protection. It is believed that an effective HSV-1 vaccine must generate both highly effective cell-mediated and humoral adaptive immune responses in order (i) to diminish infectivity, (ii) to limit replication, (iii) to reduce local and neurotropic spread, and (iv) to maintain disseminated virus in a latent state within the peripheral nervous system. Because animals vaccinated with HSV-1 0ΔNLS displayed such characteristics of protection upon challenge without experiencing consequential ocular pathology, the adaptive immune responses were compared among all experimental groups to extrapolate the respective correlates of protection.

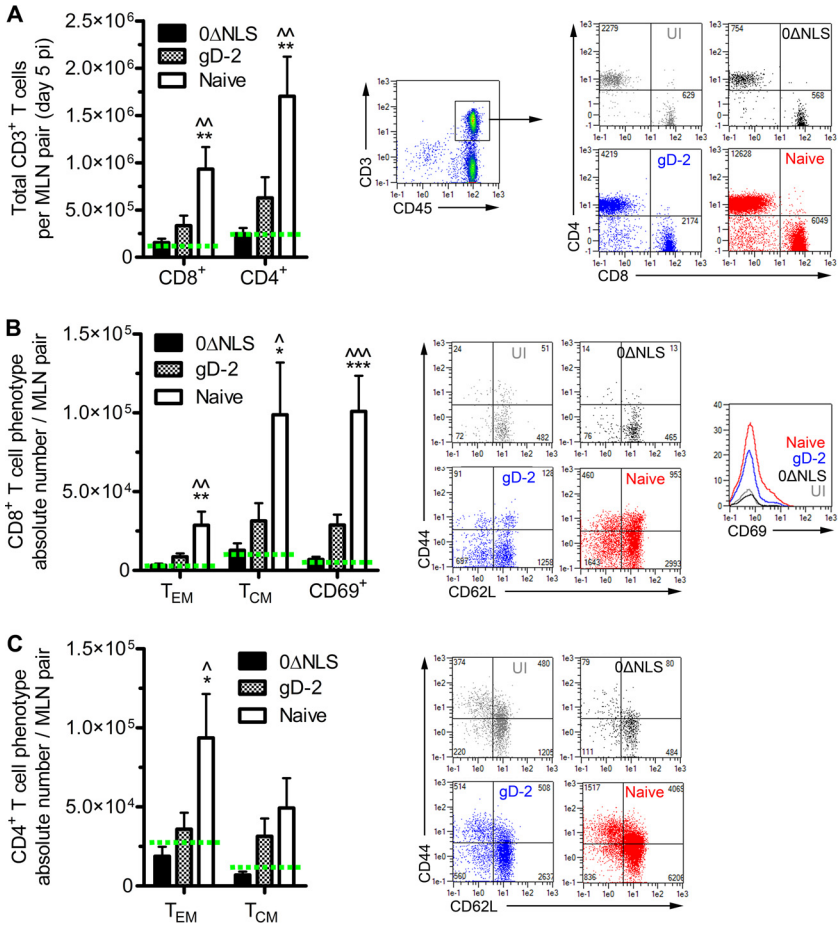

FIG 5 Host adaptive immune response in the local draining lymph nodes. (A) Generation of an adaptive cellular immune response in the local draining (mandibular) lymph nodes (MLN) was assessed by flow cytometry to evaluate expansion of $CD4^+$ and $CD8^+$ T cells following ocular HSV-1 infection ($n = 9$ to 10 mice/group; 3 independent experiments). (B) The total $CD8^+$ T cell populations shown in panel A were subgated to phenotypically characterize the effector memory (T_{EM}; $CD44^+$ $CD62L^-$) or central memory (T_{CM}; $CD44^+$ $CD62L^+$) subsets and quantify activated ($CD69^+$) cells. (C) The total $CD4^+$ T cell populations shown in panel A were also subgated to phenotypically characterize the T_{EM} and T_{CM} subsets. Representative flow plots are shown for each group. Significance thresholds for all panels are indicated as follows: */^, $P < 0.05$; **/^^, $P < 0.01$; ***/^^^, $P < 0.001$. Significant differences in results relative to the 0ΔNLS- and the gD-2-immunized groups are shown as asterisks and carets, respectively. Green dashed lines signify the average UI value for each population.

Flow cytometry was utilized to evaluate the T lymphocyte profiles in the cornea-draining mandibular lymph nodes (MLN) and spleen as representatives of local and systemic cell-mediated immune responses to HSV-1 challenge at day 5 p.i. Profiles of $CD4^+$ and $CD8^+$ T cells within the MLN of nonvaccinated animals showed a profound expansion relative to those of UI and vaccinated mice (Fig. 5A). Lymphocyte responses were phenotypically characterized further by expression of CD44 and CD62L or CD69 into effector memory (T_{EM}; $CD44^+$ $CD62L^-$), central memory (T_{CM}; $CD44^+$ $CD62L^+$), and activated ($CD69^+$) subsets. These $CD4^+$ and $CD8^+$ T cell subset profiles were also significantly elevated in the MLN of naive mice relative to levels in all other groups (Fig. 5B and C).

Interestingly, there were no differences in any of the T cell profiles in the MLN of 0ΔNLS-vaccinated mice relative to those of UI mice, whereas gD-2-vaccinated mice exhibited 2- to 3-fold increases compared to levels in 0ΔNLS-vaccinated mice (Fig. 5A to C). However, these trends in absolute cell counts fell below significance thresholds compared by ANOVA alongside differences in naive mice. Of note, there was a significant increase ($P <$ 0.05) in the number of activated ($CD69^+$) $CD8^+$ T cells in gD-2-vaccinated mice compared to that in 0ΔNLS-vaccinated mice on a frequency (percentage of population) basis (Fig. 5B, inset histogram; numerical data not shown). Regulatory T cells (T_{reg}), defined as $CD4^+$ $CD25^+$ $FoxP3^+$, were also assessed in the MLN at day 5 p.i.; a 2- to 3-fold increase in the T_{reg} population was observed in UI mice compared to that in naive mice, whereas no expansion in the T_{reg} pool in 0ΔNLS- or gD-2 vaccinated mice was detected relative to the level in UI mice (data not shown). No differences in total numbers of splenic $CD4^+$/$CD8^+$ T cells or their phenotypically segregated T_{EM}/T_{CM} subpopulations were observed among any experimental groups or relative to levels in UI samples at day 5 p.i. (data not shown). Taken together, these results are consistent with the viral titers recovered in mice following challenge (Fig. 2D to F) as more viral antigen would be accessible to stimulate local immune responses in mice with elevated tissue viral loads. Moreover, these results also demonstrate that protection against ocular HSV-1 infection can be mediated in vaccinated hosts without compromising corneal health or provoking immune responses upon challenge that, in turn, may

contribute to immunoinflammatory pathologies and threaten visual acuity.

Since T lymphocyte recall responses in secondary lymphoid organs did not correlate with viral clearance and protection in 0ΔNLS-vaccinated mice, neutralizing antibody titers were evaluated. Serum obtained from naive mice had no detectable capacity to neutralize the infectivity of HSV-1 virions. Serum from gD-2-vaccinated mice exhibited modest neutralizing capacity, but this was overshadowed by the significantly greater potency of 0ΔNLS antiserum in both postprimary and postboost samples (Fig. 6A). Specifically, 0ΔNLS antiserum was 28- and 12-fold more potent in its virus neutralization capacity than gD-2 antiserum in postprimary and postboost samples, respectively.

To accompany serum neutralization data, Western blotting was used to assess the specificity and breadth of viral proteins recognized by serum from immunized mice. In alignment with previous observations (32), serum from gD-2-vaccinated mice recognized a protein consistent with the size of HSV-1 gD (Fig. 6B). Moreover, serum from 0ΔNLS-vaccinated mice recognized multiple proteins recovered from HSV-1-infected Vero cell lysates (Fig. 6B), consistent with this vaccine's antigenic breadth (Fig. 1A). To determine what fraction of 0ΔNLS serum was directed against glycoprotein D, the immunoreactivities of gD-2 and 0ΔNLS antisera (Fig. 6C) were compared by Western blotting. Naive serum exhibited negligible reactivity in Western blotting (data not shown). Serum from gD-2-immunized mice did not react with proteins in uninfected (UI) Vero cells and exclusively targeted the mature (55-kDa) and immature (58-kDa) forms of gD expressed by HSV-1 (KOS) (Fig. 6C). Lysates from cells infected with an HSV-1 ΔgD mutant virus did not express any proteins that significantly reacted with gD-2 antiserum. In contrast, gD-2 antiserum significantly reacted with the mature and immature forms of gD expressed by HSV-2 (strain MS) and similarly reacted with a Vero cell line, TR-gD-2, that stably expresses the gD-2 protein (Fig. 6C). In contrast, serum from 0ΔNLS-immunized mice reacted with at least eight different proteins in the molecular mass range of 65 to 300 kDa (Fig. 6C). Importantly, an HSV-1 ΔgD mutant virus expressed all eight of the same dominant antigens that were targeted by antibodies in 0ΔNLS antiserum, hence signifying that the majority of antibodies in 0ΔNLS antiserum do not target the 55-kDa gD protein (Fig. 6C). Consistent with this interpretation, very little of the antibody in 0ΔNLS antiserum reacted with the gD-2 protein that was over expressed in the stable TR-gD-2 cell line (Fig. 6C). The 0ΔNLS antibody response was relatively type specific as the many antibodies that reacted with HSV-1 (KOS) proteins failed to react strongly with the homologous proteins encoded by wild-type HSV-2 (strain MS) (Fig. 6C). Such observations suggest that the 0ΔNLS vaccine would be a far more effective HSV-1 vaccine than a similarly designed live HSV-2 vaccine as live HSV-1 and HSV-2 vaccines appear to elicit strongly serotype-biased immune responses.

Passive immunization and viral pathogenesis. Passive transfer experiments were undertaken to determine whether serum from vaccinated mice could protect naive recipients from HSV-1 challenge. A single bolus of serum was administered to naive mice via intraperitoneal injection 24 h prior to HSV-1 challenge, and animals were monitored for survival. The results clearly support the protective efficacy of the serum from 0ΔNLS-vaccinated animals in which 90% (18/20) of recipient mice survived infection whereas only 65% (13/20) of gD-2 serum-treated (serum-Tx) recipients and 46% (6/13) of naive serum-Tx recipients survived to day 30 p.i. (Fig. 7A). Cumulative survival data show that passive immunization can limit viral pathogenesis sufficiently to alleviate mortality resulting from viral encephalitis (50).

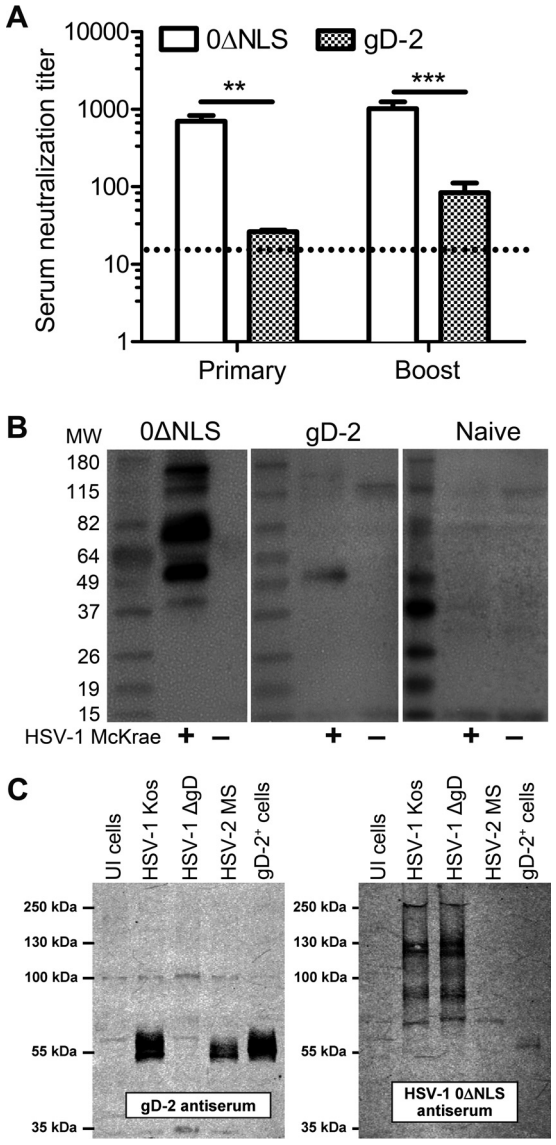

FIG 6 Humoral immune response. (A) Virus neutralization capacity of serum from immunized animals, with 1 neutralizing unit defined as the concentration of serum that prevents 50% CPE on Vero cell monolayers (MOI of ≈1.5; $n = 18$ to 20 mice per group; 5 independent experiments). Neutralizing titers were not observed with serum obtained from naive mice. The dotted line indicates the level of detection (1:12.5; assay threshold, 1:3,200). Significance thresholds were determined by Student's t tests comparing 0ΔNLS to gD-2 samples and are indicated as follows: *, $P < 0.01$; **, $P < 0.001$. (B) Representative Western blots showing the breadth of viral proteins recognized in serum from immunized and naive mice. Lysates were resolved on polyacrylamide gels and probed with a 1:500 dilution of serum. The breadth of humoral responses was based on the number of reactive bands on lysates from uninfected (UI) or HSV-1 (McKrae)-infected Vero cells. (C) Western blots showing specificity of gD-2 and 0ΔNLS serum. Cell lysates from UI cells or cells infected with wild-type HSV-1 (KOS), HSV-1 deficient in gD (ΔgD), wild-type HSV-2 (strain MS), or TR-gD-2 cells expressing gD-2 (gD-2$^+$) were resolved on polyacrylamide gels and probed with serum from gD-2- or 0ΔNLS-vaccinated mice at a 1:5,000 dilution. MW, molecular weight (in thousands).

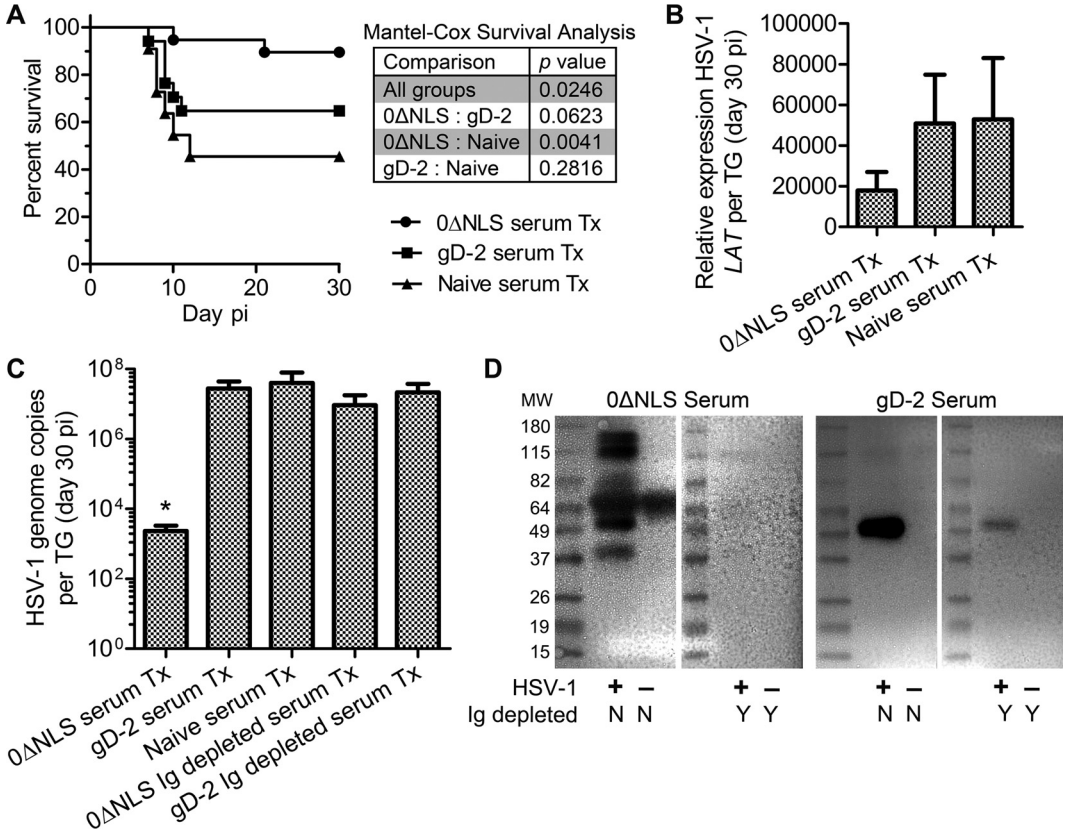

FIG 7 Passive immunization outcome measures. (A) Animal survival following HSV-1 infection comparing mice passively immunized with 0ΔNLS and gD-2 serum to a naive control group ($n = 13$ to 20 mice per group; 4 to 5 independent experiments). Significance thresholds were calculated using the Mantel-Cox test (log rank) to compare differences in survival outcomes (P values in inset table). (B) Viral latency in TG from passively immunized mice measured by expression of HSV-1 *LAT* relative to *GAPDH* and *Eef1e1* expression ($n = 4$ naive and 14 to 16 vaccine serum-Tx mice per group; 3 to 4 independent experiments). (C) The HSV-1 DNA genome copy number was evaluated by PCR in TG from passively immunized mice treated with Ig-replete 0ΔNLS, gD-2, or naive mouse serum or with Ig-depleted 0ΔNLS/gD-2 serum ($n = 6$ to 15 Ig-replete serum-Tx mice per group and 3 to 5 Ig-depleted serum-Tx mice per group; 3 to 4 independent experiments). The assay's upper limit of detection was 1×10^8 copies. Differences in HSV-1 genome copy numbers were determined by nonparametric Kruskal-Wallis ANOVA with Dunn's multiple comparison tests (*,$P < 0.05$). (D) Representative Western blots shown were used to confirm the efficiency of Ig depletion (N/Y, no/yes) based on serum reactivity against UI and HSV-1 (McKrae)-infected Vero cell lysates resolved on polyacrylamide gels. MW, molecular weight (in thousands).

The reservoir of latent HSV-1 in the TG of surviving, passively immunized animals at day 30 p.i. was subsequently evaluated by RT-PCR amplification of *LAT* and by quantitative PCR assessing the number of viral genome copies. Trends in *LAT* expression suggested a 50% reduction in 0ΔNLS serum-Tx mice relative to that in gD-2 or naive serum-Tx mice (Fig. 7B). However, a more sensitive assay was utilized to quantify HSV-1 genome copy number due to the observed variability in *LAT* expression. Data show that the copy number was reduced by more than 4 orders of magnitude in 0ΔNLS serum-Tx mice than in gD-2 or naive serum-Tx mice (Fig. 7C). To verify the role of immunoglobulin (Ig) rather than soluble factors with respect to reduction of latent HSV-1, TG were collected from mice passively immunized with Ig-depleted serum. As hypothesized, TG from 0ΔNLS Ig-depleted serum-Tx and gD-2 Ig-depleted serum-Tx mice harbored the same magnitude of HSV-1 genome as observed in gD-2 serum-Tx or naive serum-Tx mice (Fig. 7C). Western blotting was used to validate the efficiency of serum Ig depletion (Fig. 7D). Passive immunization with the high-neutralizing-titer 0ΔNLS antiserum largely prevented animals from succumbing to HSV-1 infection and significantly reduced the establishment of viral latency (Fig. 7A to C). Furthermore, this protective effect was eliminated in mice treated with Ig-depleted serum (Fig. 7C). This last point was underscored by an increase in mortality in mice passively immunized with Ig-depleted 0ΔNLS serum, with 50% of the immunized mice succumbing to infection (data not shown). Thus, the data demonstrate that antibody is a primary source of resistance to ocular challenge, thereby confirming that humoral immunity is a strong correlate of protection against HSV-1 pathogenesis and latency. Nevertheless, protection against viral neuro-dissemination and latency does not guarantee protection from ocular pathology.

Passive immunization and ocular pathology. Passively immunized mice surviving the ocular challenge displayed noticeable changes in appearance in tissue surrounding the eye. Specifically, naive and gD-2 serum-treated mice consistently displayed scabs and lesions on the eyelids and tissue proximal to the eyes at day 30 p.i. (Fig. 8A). In contrast, the vast majority of 0ΔNLS serum-treated mice assumed an uninfected appearance by day 30 p.i., with little to no noticeable changes in tissue surrounding the eye (Fig. 8A). Consistent with these results, when virus shedding in the tear film was evaluated on days 3, 5, and 7 p.i. in passively immunized mice, a significant reduction in HSV-1 shedding was

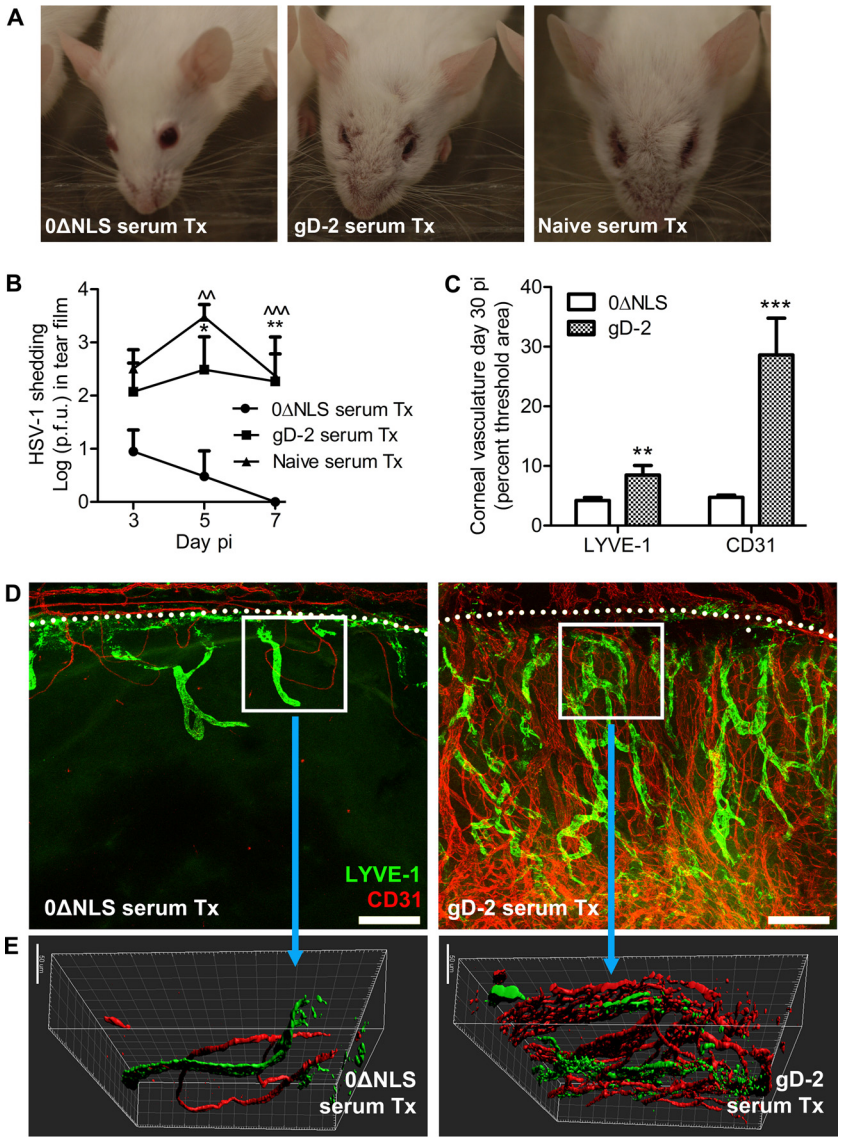

FIG 8 Ocular protection elicited by passive immunization. (A) Representative photograph of mice surviving to day 30 p.i. passively immunized (i.e., treated, Tx) with serum from naive, gD-2 subunit-vaccinated, or 0ΔNLS-vaccinated mice. (B) Viral shedding in the ocular tear film was evaluated at the indicated times p.i. in passively immunized mice ($n = 5$ mice per group; 2 independent experiments). (C) Pathological corneal neovascularization was evaluated by confocal microscopy as described in the legend of Fig. 4. The total area of $CD31^+$ blood vessels and LYVE-1^+ lymphatic vessels in the cornea quantified using MetaMorph software is shown. Differences in vessels were determined using Student's *t* tests ($n = 4$ to 6 mice per group; 2 independent experiments). Significance thresholds are designated as follows: *, $P < 0.01$; **, $P < 0.001$. (D) Representative images of quantified data showing corneal neovascularization in each group (magnification, ×10; scale bar, 200 μm). Dotted lines indicate the limbus, the naturally vascularized anatomic boundary circumscribing the healthy cornea. (E) Multidimensional reconstruction of boxed areas in panel D depicting density and depth of cornea-infiltrating blood and lymphatic vessels (magnification, ×40; scale bar, 50 μm).

observed at days 3 and 5 p.i. in 0ΔNLS serum-Tx mice relative to levels of shedding in gD-2 serum-Tx or naive serum-Tx mice (Fig. 8B). Furthermore, no virus was detectible in cornea swabs by day 7 p.i. in 0ΔNLS serum-Tx mice (Fig. 8B), consistent with the observed reduction in latent virus by day 30 p.i. (Fig. 7B and C).

Since unabated corneal HSV-1 infection initiates inflammatory responses that mediate corneal neovascularization (41), we assessed corneal hemangiogenesis and lymphangiogenesis by confocal microscopy in passively immunized mice. Mice treated with gD-2 serum exhibited profound corneal neovascularization by day 30 p.i., whereas corneas in 0ΔNLS serum-Tx mice appeared relatively healthy in comparison (Fig. 8C and D). Corneas of 0ΔNLS serum-Tx mice featured only minor ingrowth of $CD31^+$ blood vessels and lymphatic vessel antigen-1 (LYVE-1^+) lymphatic vessels from the limbus into the cornea proper (Fig. 8D). Multidimensional reconstruction of corneas imaged at higher magnification shows that the $CD31^+$ vessels not only occupy a greater area of the cornea (as shown in Fig. 8E) but also penetrate deeper into the corneal stroma (Fig. 8E). These data further substantiate the protective role of antibody in limiting ocular HSV-1 infection as we now show that corneal neovascularization pursuant to HSV-1 challenge can essentially be abrogated through pas-

sive immunization with serum possessing high neutralizing titers. Our data collectively and definitively show that highly neutralizing virus-specific antibody is essential for protection against HSV-1 pathogenesis and latency and prevention of corneal pathology.

DISCUSSION

We have compared the protection elicited from the gD-2 and 0ΔNLS vaccines in a murine ocular HSV-1 infection model. The results show that a strong correlate of protection against both HSV-1 pathogenesis and ocular pathology is prophylactic vaccine-mediated humoral immunity. Furthermore, our data demonstrate that an efficacious prophylactic vaccine can elicit a sufficiently protective threshold of humoral immunity against HSV-1 that prevents expansion of T cells in draining lymph nodes upon viral challenge and prevents corneal immunopathology. This differs from the immune response observed in a naive host in which a T cell dominant response is generated, but corneal pathology ensues as a consequence. The 0ΔNLS vaccine elicits superior protection over gD-2 as the former inhibits viral replication in the ocular mucosae and diminishes establishment of latent infection in the TG more efficiently than the latter. It comes as no surprise that a live attenuated virus would elicit better immunologic protection against viral pathogenesis than an adjuvanted glycoprotein subunit vaccine (11, 28, 32, 51). What is novel in the present investigation and a significant advancement within the arena of HSV-1 vaccine research is the formal demonstration of humoral immunity as a strong component of protection against HSV-1 pathogenesis and latency and resultant ocular disease.

Results from the recent Herpevac Trial for Women revealed that the gD-2 subunit vaccine elicited moderately efficacious cross-protection (58%) against development of culture-positive HSV-1 genital disease in a longitudinal study involving a cohort of healthy HSV-1/2-seronegative individuals (36, 52). Protection against clinical disease was linked to the quality of the subject's humoral immune response, specifically, the production and potency of several virus-neutralizing antibody clones recognizing distinct conformational epitopes on gD (52–54). The amino acid sequences for gDs from HSV-1/2 are 84% homologous (52). However, the ability of an antibody to bind surface glycoproteins on intact virions not only is a matter of affinity but also is contingent upon the structural dynamics of the virion. Interactions among HSV surface glycoproteins (e.g., gD and gC/E) during host cell attachment and fusion introduce steric hindrances and thereby affect anti-gD antibody avidity and neutralization capacity against HSV-2 but not HSV-1 *in vitro* (54). Epitope shielding is likely not a phenomenon exclusive to antibodies directed against gD-2 but, rather, an inevitable outcome of single-subunit vaccines. Accordingly, we advocate for the use of a live attenuated HSV-1 vaccine to increase the breadth of antigenic targets.

Our results also have important implications for HSV vaccine development with respect to optimization of immunization strategies. Explicitly, the immune response generated from vaccination with gD-2 adjuvanted with alum and MPL is insufficient to combat HSV-1 infection within a mucosal site to the extent required to curtail viral neuroinvasion and establishment of latency. While a 4-fold increase in humoral protection over background is generally accepted as a protective margin for vaccine efficacy, this arbitrary threshold may be insufficient for protection against HSV-1. Results from the current investigation clearly show that virus-neutralizing serum antibody titers generated from vaccination with 0ΔNLS are 12- to 28-fold higher than what can be achieved with current gD-2 subunit vaccines. Vaccine-mediated protection against mucosal pathogens is generally mediated by perfusion of that site with an adequate concentration of pathogen-neutralizing antibody that, in the instance of HSV-1, would involve counteracting local replication, dissemination, and resultant clinical disease following infection (51). Overall antibody titers, specifically IgG, in healthy external mucosal sites such as the cornea and ocular tear film are significantly reduced compared to serum titers and therefore are likely insufficient to completely prevent infection (51, 55, 56). However, IgG perfusion into the cornea and tears can increase sharply following ocular infection (55). We speculate that this process may be the primary means by which 0ΔNLS-vaccinated mice control local ocular infection.

The functional effect of various adjuvants on the development of adaptive immune responses continues to be an area of active investigation (57). Vaccines adjuvanted with alum combined with MPL, such as the gD-2 subunit vaccine, have been shown (i) to stimulate T_h1-skewed responses, (ii) to enhance cytotoxic $CD8^+$ T cell function, and (iii) to amplify and sustain humoral immunity; all of these responses are mechanistic outcomes of Toll-like receptor 4 (TLR4)-dependent cytokine production spurring proficient antigen-presenting cell activation (58–61). Humoral responses from subunit vaccines typically require restimulation of memory B cells through a secondary immunization to generate long-lived, antibody-secreting plasma cells (51). Live attenuated viruses used as vaccines also stimulate innate immune responses through host pattern recognition receptor signaling pathways in order to drive potent adaptive immune responses involving both T and B cell compartments, usually leading to efficacious humoral immunity with a single dose (51). While the current investigation has focused on humoral protection elicited by 0ΔNLS, we do not dismiss the ability of this vaccine to generate T cell responses to HSV-1 as T cell responses in the corneas of 0ΔNLS-vaccinated mice were elevated (Fig. 3E).

Many endeavors have sought to generate a combined B and T cell-based HSV vaccine for prophylactic and therapeutic use as tissue-resident memory (T_{RM}) $CD8^+$ T cells are responsible for maintaining HSV-1 in a latent state once infection is established in peripheral nerve ganglia (23, 24). Animal studies indicate that gD-2 vaccines adjuvanted with alum alone were less protective than gD-2 vaccines combined with MPL in generating protective responses against disease as a result of HSV-2 reactivation (62). However, the effectiveness of memory T cell generation induced by vaccination is ultimately dependent upon the recall potential of these cells. Rapid innate-like kinetics can be observed among subsets of antigen-experienced memory $CD8^+$ T cells within secondary lymphoid organs as well as T_{RM} $CD8^+$ T cells with regard to recall effector functions upon reexposure to antigen (63–65). In contrast, central memory $CD8^+$ T cells possess excellent proliferation potential with delayed effector function (63–65). In scenarios of acute viral replication in a site not primed with T_{RM} cells, such as the cornea during HSV-1 challenge in prophylactically immunized mice, T cells in peripheral lymphoid organs must be activated via restimulation and must proliferate and migrate to the site of infection to mediate pathogen clearance. T cell activation was not observed in secondary lymphoid organs upon ocular HSV-1 challenge in 0ΔNLS-vaccinated mice, likely due to (i) the efficiency of antibody-mediated viral clearance, (ii) the lack of

viral antigen, and, perhaps, (iii) the stimulation of innate immune pathways below the threshold required to terminate corneal immune privilege and activate antigen-presenting cells.

Vaccine-mediated protection in our model enables maintenance of corneal angiogenic privilege. The pericorneal vasculature contributes to homeostasis of ocular immune privilege (66), and our data show that 0ΔNLS-vaccinated mice are spared from pathological corneal neovascularization following HSV-1 challenge in an antibody-dependent manner. Moreover, we also report preservation of corneal nerve sensitivity in challenged mice. This novel insight is relevant as neurogenic maintenance of immune privilege has also been suggested (67, 68). Further substantiating the interplay of vaccine-mediated correlates of protection and prevention of ocular disease will also provide a basis for the development of vaccines or therapies for use against other ocular pathogens.

The correlates of immunologic protection for most vaccines have been traditionally dichotomized into either neutralizing antibody or T cell responses. However, effective antibody-dependent cellular cytotoxicity (ADCC) as an secondary correlate of humoral immunity has been gaining traction recently according to the premise that neutralizing antibody is necessary yet insufficient for protection against some viral infections (69). Furthermore, IFN-driven antiviral effectors such as tetherin, which we have recently shown to be essential for restricting local spread and neuroinvasion in HSV-1-infected corneas (70), may also enhance ADCC (71, 72). Further investigation into mechanisms of 0ΔNLS-mediated protection utilizing the genetic and immunologic tools available with inbred C57BL/6 mice is ongoing. In summary, our data collectively show for the first time (i) that vaccine-mediated protection against ocular HSV-1-associated disease can be achieved using multiple quantifiable and clinically relevant measures, (ii) that a correlate of protection against HSV-1 pathogenesis and latency is preexisting humoral immunity, and (iii) that immune responses thought to mediate ocular pathology as a consequence of viral clearance in the cornea can be averted by prophylactic vaccination with a highly efficacious vaccine, 0ΔNLS.

ACKNOWLEDGMENTS

We thank Meghan Carr for technical assistance, the Dean McGee Eye Institute vivarium staff for maintaining our animals, Brian Gebhardt for supplying the original stock of HSV-1 McKrae, and Edward Gershburg for furnishing the recombinant gD-2_{306t} protein.

D.J.R. designed and conducted experiments, analyzed all data, and prepared the manuscript; H.R.G. performed confocal imaging; J.K.J. performed serum neutralization assays and Western blotting and assisted with PCR experiments; J.J.G. performed Western blotting and assisted in interpretation of results; J.L.W. evaluated and scored mice for opacity; W.P.H. designed the 0ΔNLS virus and critiqued the manuscript; and D.J.J.C. conducted experiments and supervised all work.

D.J.R., H.R.G., J.K.J., J.J.G, J.L.W., and D.J.J.C. have no conflicts of interest to report. W.P.H. is a coauthor on U.S. patent 8802109, which describes the uses of herpes simplex virus mutant ICP0 in the design of a live attenuated HSV-2 vaccine strain. In addition, W.P.H. is a cofounder of Rational Vaccines, Inc., which has licensed U.S. patents 77856605 and 8802109.

The content of the manuscript is solely the responsibility of the authors and does not necessarily represent the official views of the National Institutes of Health or the National Eye Institute.

FUNDING INFORMATION

This work, including the efforts of Daniel J. J. Carr, was funded by Research to Prevent Blindness (RPB) (unrestricted grant). This work, including the efforts of Daniel J. J. Carr, was funded by HHS | NIH | National Eye Institute (NEI) (R01 EY021238, T32 EY023202, and P30 EY021725).

REFERENCES

1. **Farooq AV, Shukla D.** 2012. Herpes simplex epithelial and stromal keratitis: an epidemiologic update. Surv Ophthalmol **57:**448–462. http://dx.doi.org/10.1016/j.survophthal.2012.01.005.
2. **Rowe AM, St Leger AJ, Jeon S, Dhaliwal DK, Knickelbein JE, Hendricks RL.** 2013. Herpes keratitis. Prog Retin Eye Res **32:**88–101. http://dx.doi.org/10.1016/j.preteyeres.2012.08.002.
3. **Egan KP, Wu S, Wigdahl B, Jennings SR.** 2013. Immunological control of herpes simplex virus infections. J Neurovirol **19:**328–345. http://dx.doi.org/10.1007/s13365-013-0189-3.
4. **Doymaz MZ, Rouse BT.** 1992. Herpetic stromal keratitis: an immunopathologic disease mediated by $CD4^+$ T lymphocytes. Invest Ophthalmol Vis Sci **33:**2165–2173.
5. **Hendricks RL, Tumpey TM, Finnegan A.** 1992. IFN-gamma and IL-2 are protective in the skin but pathologic in the corneas of HSV-1-infected mice. J Immunol **149:**3023–3028.
6. **Thomas J, Gangappa S, Kanangat S, Rouse BT.** 1997. On the essential involvement of neutrophils in the immunopathologic disease: herpetic stromal keratitis. J Immunol **158:**1383–1391.
7. **Lepisto AJ, Frank GM, Xu M, Stuart PM, Hendricks RL.** 2006. CD8 T cells mediate transient herpes stromal keratitis in CD4-deficient mice. Invest Ophthalmol Vis Sci **47:**3400–3409. http://dx.doi.org/10.1167/iovs.05-0898.
8. **Divito SJ, Hendricks RL.** 2008. Activated inflammatory infiltrate in HSV-1-infected corneas without herpes stromal keratitis. Invest Ophthalmol Vis Sci **49:**1488–1495. http://dx.doi.org/10.1167/iovs.07-1107.
9. **Suryawanshi A, Veiga-Parga T, Rajasagi NK, Reddy PBJ, Sehrawat S, Sharma S, Rouse BT.** 2011. Role of IL-17 and Th17 cells in herpes simplex virus-induced corneal immunopathology. J Immunol **187:**1919–1930. http://dx.doi.org/10.4049/jimmunol.1100736.
10. **Conrady CD, Zheng M, Stone DU, Carr DJJ.** 2012. $CD8^+$ T cells suppress viral replication in the cornea but contribute to VEGF-C-induced lymphatic vessel genesis. J Immunol **189:**425–432. http://dx.doi.org/10.4049/jimmunol.1200063.
11. **Royer DJ, Cohen AW, Carr DJ.** 2015. The current state of vaccine development for ocular HSV-1 infection. Expert Rev Ophthalmol **10:**113–126. http://dx.doi.org/10.1586/17469899.2015.1004315.
12. **Ghiasi H, Bahri S, Nesburn AB, Wechsler SL.** 1995. Protection against herpes simplex virus-induced eye disease after vaccination with seven individually expressed herpes simplex virus 1 glycoproteins. Invest Ophthalmol Vis Sci **36:**1352–1360.
13. **Ghiasi H, Nesburn AB, Wechsler SL.** 1996. Vaccination with a cocktail of seven recombinantly expressed HSV-1 glycoproteins protects against ocular HSV-1 challenge more efficiently than vaccination with any individual glycoprotein. Vaccine **14:**107–112. http://dx.doi.org/10.1016/0264-410X(95)00169-2.
14. **Keadle TL, Laycock KA, Miller JK, Hook KK, Fenoglio ED, Francotte M, Slaoui M, Stuart PM, Pepose JS.** 1997. Efficacy of a recombinant glycoprotein D subunit vaccine on the development of primary and recurrent ocular infection with herpes simplex virus type 1 in mice. J Infect Dis **176:**331–338. http://dx.doi.org/10.1086/514049.
15. **Inoue T, Inoue Y, Nakamura T, Yoshida A, Takahashi K, Inoue Y, Shimomura Y, Tano Y, Fujisawa Y, Aono A, Hayashi K.** 2000. Preventive effect of local plasmid DNA vaccine encoding gD or gD-IL-2 on herpetic keratitis. Invest Ophthalmol Vis Sci **41:**4209–4215.
16. **Stanberry LR, Bernstein DI, Burke RL, Pachl C, Myers MG.** 1987. Vaccination with recombinant herpes simplex virus glycoproteins: protection against initial and recurrent genital herpes. J Infect Dis **155:**914–920. http://dx.doi.org/10.1093/infdis/155.5.914.
17. **Berman PW, Vogt PE, Gregory T, Lasky LA, Kern ER.** 1988. Efficacy of recombinant glycoprotein D subunit vaccines on the development of primary, recurrent, and latent genital infections with herpes simplex virus type 2 in guinea pigs. J Infect Dis **157:**897–902. http://dx.doi.org/10.1093/infdis/157.5.897.
18. **van Lint AL, Torres-Lopez E, Knipe DM.** 2007. Immunization with a replication-defective herpes simplex virus 2 mutant reduces herpes sim-

plex virus 1 infection and prevents ocular disease. Virology **368:**227–231. http://dx.doi.org/10.1016/j.virol.2007.08.030.
19. **Orr MT, Orgun NN, Wilson CB, Way SS.** 2007. Cutting edge: recombinant Listeria monocytogenes expressing a single immune-dominant peptide confers protective immunity to herpes simplex virus-1 infection. J Immunol **178:**4731–4735. http://dx.doi.org/10.4049/jimmunol.178.8.4731.
20. **Lu Z, Brans R, Akhrameyeva NV, Murakami N, Xu X, Yao F.** 2009. High-level expression of glycoprotein D by a dominant-negative HSV-1 virus augments its efficacy as a vaccine against HSV-1 infection. J Investig Dermatol **129:**1174–1184. http://dx.doi.org/10.1038/jid.2008.349.
21. **Hu K, Dou J, Yu F, He X, Yuan X, Wang Y, Liu C, Gu N.** 2011. An ocular mucosal administration of nanoparticles containing DNA vaccine pRSC-gD-IL-21 confers protection against mucosal challenge with herpes simplex virus type 1 in mice. Vaccine **29:**1455–1462. http://dx.doi.org/10.1016/j.vaccine.2010.12.031.
22. **Keadle TL, Morrison LA, Morris JL, Pepose JS, Stuart PM.** 2002. Therapeutic immunization with a virion host shutoff-defective, replication-incompetent herpes simplex virus type 1 strain limits recurrent herpetic ocular infection. J Virol **76:**3615–3625. http://dx.doi.org/10.1128/JVI.76.8.3615-3625.2002.
23. **Liu T, Khanna KM, Chen X, Fink DJ, Hendricks RL.** 2000. $CD8^+$ T cells can block herpes simplex virus type 1 (HSV-1) reactivation from latency in sensory neurons. J Exp Med **191:**1459–1466. http://dx.doi.org/10.1084/jem.191.9.1459.
24. **Khanna KM, Bonneau RH, Kinchington PR, Hendricks RL.** 2003. Herpes simplex virus-specific memory $CD8^+$ T cells are selectively activated and retained in latently infected sensory ganglia. Immunity **18:**593–603. http://dx.doi.org/10.1016/S1074-7613(03)00112-2.
25. **Knickelbein JE, Khanna KM, Yee MB, Baty CJ, Kinchington PR, Hendricks RL.** 2008. Noncytotoxic lytic granule-mediated $CD8^+$ T cell inhibition of HSV-1 reactivation from neuronal latency. Science **322:**268–271. http://dx.doi.org/10.1126/science.1164164.
26. **Srivastava R, Khan AA, Huang J, Nesburn AB, Wechsler SL, BenMohamed L.** 2015. A herpes simplex virus type 1 human asymptomatic $CD8^+$ T-cell epitopes-based vaccine protects against ocular herpes in a "humanized" HLA transgenic rabbit model. Invest Ophthalmol Vis Sci **56:**4013–4028. http://dx.doi.org/10.1167/iovs.15-17074.
27. **Ghiasi H, Wechsler SL, Cai S, Nesburn AB, Hofman FM.** 1998. The role of neutralizing antibody and T-helper subtypes in protection and pathogenesis of vaccinated mice following ocular HSV-1 challenge. Immunology **95:**352–359. http://dx.doi.org/10.1046/j.1365-2567.1998.00602.x.
28. **Plotkin SA.** 2010. Correlates of protection induced by vaccination. Clin Vaccine Immunol **17:**1055–1065. http://dx.doi.org/10.1128/CVI.00131-10.
29. **St Leger AJ, Peters B, Sidney J, Sette A, Hendricks RL.** 2011. Defining the herpes simplex virus-specific $CD8^+$ T cell repertoire in C57BL/6 mice. J Immunol **186:**3927–3933. http://dx.doi.org/10.4049/jimmunol.1003735.
30. **Lanfranca M, Mostafa H, Davido D.** 2014. HSV-1 ICP0: an E3 ubiquitin ligase that counteracts host intrinsic and innate Immunity. Cells **3:**438–454. http://dx.doi.org/10.3390/cells3020438.
31. **Halford WP, Püschel R, Rakowski B.** 2010. Herpes simplex virus 2 ICP0 mutant viruses are avirulent and immunogenic: implications for a genital herpes vaccine. PLoS One **5:**e12251. http://dx.doi.org/10.1371/journal.pone.0012251.
32. **Halford WP, Püschel R, Gershburg E, Wilber A, Gershburg S, Rakowski B.** 2011. A live-attenuated HSV-2 *ICP0*$^-$ virus elicits 10 to 100 times greater protection against genital herpes than a glycoprotein D subunit vaccine. PLoS One **6:**e17748. http://dx.doi.org/10.1371/journal.pone.0017748.
33. **Liu M, Schmidt EE, Halford WP.** 2010. ICP0 dismantles microtubule networks in herpes simplex virus-infected cells. PLoS One **5:**e10975. http://dx.doi.org/10.1371/journal.pone.0010975.
34. **Everett RD.** 2000. ICP0, a regulator of herpes simplex virus during lytic and latent infection. Bioessays **22:**761–770. http://dx.doi.org/10.1002/1521-1878(200008)22:8<761::AID-BIES10>3.0.CO;2-A.
35. **Sacks WR, Schaffer PA.** 1987. Deletion mutants in the gene encoding the herpes simplex virus type 1 immediate-early protein ICP0 exhibit impaired growth in cell culture. J Virol **61:**829–839.
36. **Belshe RB, Leone PA, Bernstein DI, Wald A, Levin MJ, Stapleton JT, Gorfinkel I, Morrow RLA, Ewell MG, Stokes-Riner A, Dubin G, Heineman TC, Schulte JM, Deal CD.** 2012. Efficacy results of a trial of a herpes simplex vaccine. N Engl J Med **366:**34–43. http://dx.doi.org/10.1056/NEJMoa1103151.
37. **Royer DJ, Zheng M, Conrady CD, Carr DJJ.** 2015. Granulocytes in ocular HSV-1 infection: opposing roles of mast cells and neutrophils. Invest Ophthalmol Vis Sci **56:**3763–3775. http://dx.doi.org/10.1167/iovs.15-16900.
38. **Samaniego LA, Neiderhiser L, DeLuca NA.** 1998. Persistence and expression of the herpes simplex virus genome in the absence of immediate-early proteins. J Virol **72:**3307–3320.
39. **Conrady CD, Zheng M, Fitzgerald KA, Liu C, Carr DJJ.** 2012. Resistance to HSV-1 infection in the epithelium resides with the novel innate sensor, IFI-16. Mucosal Immunol **5:**173–183. http://dx.doi.org/10.1038/mi.2011.63.
40. **Chucair-Elliott AJ, Zheng M, Carr DJJ.** 2015. Degeneration and regeneration of corneal nerves in response to HSV-1 infection. Invest Ophthalmol Vis Sci **56:**1097–1107. http://dx.doi.org/10.1167/iovs.14-15596.
41. **Wuest TR, Carr DJJ.** 2010. VEGF-A expression by HSV-1-infected cells drives corneal lymphangiogenesis. J Exp Med **207:**101–115. http://dx.doi.org/10.1084/jem.20091385.
42. **Härle P, Sainz B, Carr DJJ, Halford WP.** 2002. The immediate-early protein, ICP0, is essential for the resistance of herpes simplex virus to interferon-alpha/beta. Virology **293:**295–304. http://dx.doi.org/10.1006/viro.2001.1280.
43. **Halford WP, Weisend C, Grace J, Soboleski M, Carr DJJ, Balliet JW, Imai Y, Margolis TP, Gebhardt BM.** 2006. ICP0 antagonizes Stat 1-dependent repression of herpes simplex virus: implications for the regulation of viral latency. Virol J **3:**44. http://dx.doi.org/10.1186/1743-422X-3-44.
44. **Bryant-Hudson KM, Chucair-Elliott AJ, Conrady CD, Cohen A, Zheng M, Carr DJJ.** 2013. HSV-1 targets lymphatic vessels in the eye and draining lymph node of mice leading to edema in the absence of a functional type I interferon response. Am J Pathol **183:**1233–1242. http://dx.doi.org/10.1016/j.ajpath.2013.06.014.
45. **Hamrah P, Cruzat A, Dastjerdi MH, Zheng L, Shahatit BM, Bayhan HA, Dana R, Pavan-Langston D.** 2010. Corneal sensation and subbasal nerve alterations in patients with herpes simplex keratitis: an in vivo confocal microscopy study. Ophthalmology **117:**1930–1936. http://dx.doi.org/10.1016/j.ophtha.2010.07.010.
46. **Yun H, Rowe AM, Lathrop KL, Harvey SAK, Hendricks RL.** 2014. Reversible nerve damage and corneal pathology in murine herpes simplex stromal keratitis. J Virol **88:**7870–7880. http://dx.doi.org/10.1128/JVI.01146-14.
47. **Conrady CD, Zheng M, Mandal NA, van Rooijen N, Carr DJJ.** 2013. IFN-α-driven CCL2 production recruits inflammatory monocytes to infection site in mice. Mucosal Immunol **6:**45–55. http://dx.doi.org/10.1038/mi.2012.46.
48. **Plotkin SA.** 2008. Vaccines: correlates of vaccine-induced immunity. Clin Infect Dis **47:**401–409. http://dx.doi.org/10.1086/589862.
49. **Perella D, Wang C, Civen R, Viner K, Kuguru K, Daskalaki I, Schmid DS, Lopez AS, Tseng HF, Newbern EC, Mascola L, Bialek SR.** 14 March 2016. Varicella vaccine effectiveness in preventing community transmission in the 2-dose era. Pediatrics **2016:**peds.2015-2802.
50. **Conrady CD, Zheng M, van Rooijen N, Drevets DA, Royer D, Alleman A, Carr DJJ.** 2013. Microglia and a functional type I IFN pathway are required to counter HSV-1-driven brain lateral ventricle enlargement and encephalitis. J Immunol **190:**2807–2817. http://dx.doi.org/10.4049/jimmunol.1203265.
51. **Plotkin S, Orenstein W, Offit.** 2013. Vaccines, 6th ed. Elsevier-Saunders, Philadelphia, Pa.
52. **Belshe RB, Heineman TC, Bernstein DI, Bellamy AR, Ewell M, van der Most R, Deal CD.** 2014. Correlate of immune protection against HSV-1 genital disease in vaccinated women. J Infect Dis **209:**828–836. http://dx.doi.org/10.1093/infdis/jit651.
53. **Whitbeck JC, Huang Z-Y, Cairns TM, Gallagher JR, Lou H, Ponce-de-Leon M, Belshe RB, Eisenberg RJ, Cohen GH.** 2014. Repertoire of epitopes recognized by serum IgG from humans vaccinated with herpes simplex virus 2 glycoprotein D. J Virol **88:**7786–7795. http://dx.doi.org/10.1128/JVI.00544-14.
54. **Awasthi S, Belshe RB, Friedman HM.** 2014. Better neutralization of herpes simplex virus type 1 (HSV-1) than HSV-2 by antibody from recipients of GlaxoSmithKline HSV-2 glycoprotein D2 subunit vaccine. J Infect Dis **210:**571–575. http://dx.doi.org/10.1093/infdis/jiu177.
55. **Preston MJ, Kernacki KA, Berk JM, Hazlett LD, Berk RS.** 1992. Kinetics

of serum, tear, and corneal antibody responses in resistant and susceptible mice intracorneally infected with *Pseudomonas aeruginosa*. Infect Immun **60:**885–891.

56. **Allansmith MR, McClellan BH.** 1975. Immunoglobulins in the human cornea. Am J Ophthalmol **80:**123–132. http://dx.doi.org/10.1016/0002-9394(75)90882-X.
57. **Reed SG, Orr MT, Fox CB.** 2013. Key roles of adjuvants in modern vaccines. Nat Med **19:**1597–1608. http://dx.doi.org/10.1038/nm.3409.
58. **Mata-Haro V, Cekic C, Martin M, Chilton PM, Casella CR, Mitchell TC.** 2007. The vaccine adjuvant monophosphoryl lipid A as a TRIF-biased agonist of TLR4. Science **316:**1628–1632. http://dx.doi.org/10.1126/science.1138963.
59. **MacLeod MKL, McKee AS, David A, Wang J, Mason R, Kappler JW, Marrack P.** 2011. Vaccine adjuvants aluminum and monophosphoryl lipid A provide distinct signals to generate protective cytotoxic memory CD8 T cells. Proc Natl Acad Sci U S A **108:**7914–7919. http://dx.doi.org/10.1073/pnas.1104588108.
60. **Giannini S, Hanon E, Moris P, Vanmechelen M, Morel S, Dessy F, Fourneau M, Colau B, Suzich J, Losonksy G.** 2006. Enhanced humoral and memory B cellular immunity using HPV16/18 L1 VLP vaccine formulated with the MPL/aluminium salt combination (AS04) compared to aluminium salt only. Vaccine **24:**5937–5949. http://dx.doi.org/10.1016/j.vaccine.2006.06.005.
61. **Didierlaurent AM, Morel S, Lockman L, Giannini SL, Bisteau M, Carlsen H, Kielland A, Vosters O, Vanderheyde N, Schiavetti F, Larocque D, Van Mechelen M, Garcon N.** 2009. AS04, an aluminum salt- and TLR4 agonist-based adjuvant system, induces a transient localized innate immune response leading to enhanced adaptive immunity. J Immunol **183:**6186–6197. http://dx.doi.org/10.4049/jimmunol.0901474.
62. **Bourne N, Milligan GN, Stanberry LR, Stegall R, Pyles RB.** 2005. Impact of immunization with glycoprotein D2/AS04 on herpes simplex virus type 2 shedding into the genital tract in guinea pigs that become infected. J Infect Dis **192:**2117–2123. http://dx.doi.org/10.1086/498247.
63. **Gubser PM, Bantug GR, Razik L, Fischer M, Dimeloe S, Hoenger G, Durovic B, Jauch A, Hess C.** 2013. Rapid effector function of memory $CD8^+$ T cells requires an immediate-early glycolytic switch. Nat Immunol **14:**1064–1072. http://dx.doi.org/10.1038/ni.2687.
64. **Masopust D, Picker LJ.** 2012. Hidden memories: frontline memory T cells and early pathogen interception. J Immunol **188:**5811–5817. http://dx.doi.org/10.4049/jimmunol.1102695.
65. **Bachmann MF, Wolint P, Schwarz K, Oxenius A.** 2005. Recall proliferation potential of memory $CD8^+$ T cells and antiviral protection. J Immunol **175:**4677–4685. http://dx.doi.org/10.4049/jimmunol.175.7.4677.
66. **Park PJ, Chang M, Garg N, Zhu J, Chang J-H, Shukla D.** 2015. Corneal lymphangiogenesis in herpetic stromal keratitis. Surv Ophthalmol **60:**60–71. http://dx.doi.org/10.1016/j.survophthal.2014.06.001.
67. **Paunicka KJ, Mellon J, Robertson D, Petroll M, Brown JR, Niederkorn JY.** 2015. Severing corneal nerves in one eye induces sympathetic loss of immune privilege and promotes rejection of future corneal allografts placed in either eye. Am J Transplant **15:**1490–1501. http://dx.doi.org/10.1111/ajt.13240.
68. **Vega JL, Keino H, Masli S.** 2009. Surgical denervation of ocular sympathetic afferents decreases local transforming growth factor-β and abolishes immune privilege. Am J Pathol **175:**1218–1225. http://dx.doi.org/10.2353/ajpath.2009.090264.
69. **Schmaljohn AL.** 2013. Protective antiviral antibodies that lack neutralizing activity: precedents and evolution of concepts. Curr HIV Res **11:**345–353. http://dx.doi.org/10.2174/1570162X113116660057.
70. **Royer DJ, Carr DJJ.** 2 December 2015. A STING-dependent innate-sensing pathway mediates resistance to corneal HSV-1 infection via up-regulation of the antiviral effector tetherin. Mucosal Immunol http://dx.doi.org/10.1038/mi.2015.124.
71. **Alvarez RA, Hamlin RE, Monroe A, Moldt B, Hotta MT, Rodriguez Caprio G, Fierer DS, Simon V, Chen BK.** 2014. HIV-1 Vpu antagonism of tetherin inhibits antibody-dependent cellular cytotoxic responses by natural killer cells. J Virol **88:**6031–6046. http://dx.doi.org/10.1128/JVI.00449-14.
72. **Arias JF, Heyer LN, von Bredow B, Weisgrau KL, Moldt B, Burton DR, Rakasz EG, Evans DT.** 2014. Tetherin antagonism by Vpu protects HIV-infected cells from antibody-dependent cell-mediated cytotoxicity. Proc Natl Acad Sci U S A **111:**6425–6430. http://dx.doi.org/10.1073/pnas.1321507111.